HEI HEALTH EFFECTS INSTITUTE

Improvement of a Respiratory Ozone Analyzer

James S. Ultman, Abdellaziz Ben-Jebria, Craig S. Mac Dougall, and Marc L. Rigas

Department of Chemical Engineering, Pennsylvania State University, University Park, PA

Includes the Commentary of the Institute's Health Review Committee

Research Report Number 79
October 1997

HEI HEALTH EFFECTS INSTITUTE

The Health Effects Institute, established in 1980, is an independent and unbiased source of information on the health effects of motor vehicle emissions. HEI studies all major pollutants, including regulated pollutants (such as carbon monoxide, ozone, nitrogen dioxide, and particulate matter), and unregulated pollutants (such as diesel engine exhaust, methanol, and aldehydes). To date, HEI has supported more than 150 projects at institutions in North America and Europe.

Typically, HEI receives half its funds from the U.S. Environmental Protection Agency and half from 28 manufacturers and marketers of motor vehicles and engines in the United States. Occasionally, funds from other public or private organizations either support special projects or provide resources for a portion of an HEI study. Regardless of funding sources, HEI exercises complete autonomy in setting its research priorities and in reaching its conclusions. An independent Board of Directors governs HEI. The Institute's Research and Review Committees serve complementary scientific purposes and draw distinguished scientists as members. The results of HEI-funded studies are made available as Research Reports, which contain both the Investigators' Report and the Review Committee's evaluation of the work's scientific quality and regulatory relevance.

HEI Statement

Synopsis of Research Report Number 79

Improvement of a Respiratory Ozone Analyzer

BACKGROUND

In many people, exposure to ozone, an irritant gas and ubiquitous air pollutant, causes reversible decreases in some measures of lung function, increases in airway reactivity, and the appearance of indicators of airway inflammation in lung fluids. Individuals having the greatest risk of developing such effects appear to be those who exercise or engage in moderate-to-strenuous physical activity. To estimate the health risk that ozone exposure may pose to humans, regulators need to know how much ozone reaches the target tissues in the respiratory tract.

Measuring respiratory dose requires an instrument that (1) can monitor ozone concentrations at the airway opening (mouth or nose) rather than in the ambient air; (2) responds dynamically at a rapid rate relative to an individual's breathing rate; and (3) is sensitive enough to measure ozone levels at or below ambient levels (0.07 to 0.20 ppm in urban areas) for both resting and exercising subjects. With previous HEI support, Dr. James Ultman and his colleagues developed a rapidly responding analyzer to measure the dose of inhaled ozone. To use it, a subject at rest inhaled air containing a predetermined bolus dose of ozone and then exhaled into the instrument, which quantified the amount of ozone exhaled. By comparing the amounts of ozone inhaled and exhaled, the investigators calculated how much ozone had been absorbed by the respiratory tract. However, this first-generation instrument proved to not be suitable for measuring ozone at levels less than 0.5 ppm or in individuals engaged in moderate-to-strenuous physical activity. HEI funded this follow-on study to improve the first-generation ozone analyzer by increasing its ozone sensitivity and its response time, thereby allowing ozone uptake to be measured at ambient levels in exercising subjects.

APPROACH

Dr. Ultman and his colleagues redesigned their first-generation analyzer to reduce electronic noise (interference) and improve the signal's stability. To do so, they adjusted each parameter that influenced the analyzer's performance: the flow of the air sample into the instrument, the pressure in the chamber where the air sample and the reactant gas mixed, the relative amounts of the reactant gas and air sample, and electronic variables (frequency and voltage). Through trial and error, they determined the combination of parameters that would produce the fastest response time, the strongest and most stable signal, and the least interference from noise. To evaluate the success of their modifications, they conducted a pilot test to measure ozone uptake in the respiratory tracts of two human subjects.

RESULTS AND IMPLICATIONS

The investigators made significant advances in improving their first-generation ozone analyzer. By redesigning that instrument, they were able to accurately measure ozone levels below 0.2 ppm. The investigators also improved the instrument's response time, even though they were unable to markedly reduce the interference from electronic noise. Further improvements in design are needed to reduce the inherent electronic noise of the instrument.

Nevertheless, because of the improved response characteristics, the second-generation ozone analyzer was able to measure ozone respiratory uptake in a pilot test using two subjects with breathing rates corresponding to moderate exercise while being exposed to 0.11 ppm ozone. In its current configuration, the instrument can be used when the subject's maximal breathing rate is 30 breaths per minute and the exposure concentration of ozone is approximately 0.1 ppm or greater. Thus, using the second-generation analyzer, more detailed clinical studies to quantify respiratory ozone uptake in exercising human subjects should be possible.

This Statement, prepared by the Health Effects Institute and approved by its Board of Directors, is a summary of a research project sponsored by HEI from 1995 to 1996. This study was conducted by Dr. James S. Ultman and colleagues of Pennsylvania State University, University Park, PA. The following Research Report contains both the detailed Investigators' Report and a Commentary on the study prepared by the Institute's Health Review Committee.

Library of Congress Catalog Number for the HEI Research Report Series: WA 754 R432.
The paper in this publication meets the minimum standard requirements of the ANSI Standard Z39.48-1984 (Permanence of Paper) effective with Report Number 21, December 1988, and with Report Numbers 25, 26, 32, 51, and 65 Parts IV, VIII, and IX excepted. These excepted Reports are printed on acid-free coated paper.

TABLE OF CONTENTS

Research Report Number 79

Improvement of a Respiratory Ozone Analyzer

James S. Ultman, Abdellaziz Ben-Jebria, Craig S. Mac Dougall, and Marc L. Rigas

Improvement of a Respiratory Ozone Analyzer

James S. Ultman, Abdellaziz Ben-Jebria, Craig S. Mac Dougall, and Marc L. Rigas

ABSTRACT

The breath-to-breath measurement of total respiratory ozone (O_3)* uptake requires monitoring O_3 concentration at the airway opening with an instrument that responds rapidly relative to the breathing frequency. Our original chemiluminescent analyzer, using 2-methyl-2-butene as the reactant gas, had a 10% to 90% step-response time of 110 msec and a minimal detectable concentration of 0.018 parts per million (ppm) O_3 (Ben-Jebria et al. 1990). This instrument was suitable for respiratory O_3 monitoring during quiet breathing and light exercise. For this study, we constructed a more self-contained analyzer with a faster response time using ethylene as the reactant gas. When the analyzer was operated at a reaction chamber pressure of 350 torr, an ethylene-to-sample flow ratio of 4:1, and a sampling flow of 0.6 liters per minute (Lpm), it had a 10% to 90% step-response time of 70 msec and a minimal detectable concentration of 0.006 ppm. These specifications make respiratory O_3 monitoring possible during moderate-to-heavy exercise. In addition, the nonlinear calibration and the carbon dioxide (CO_2) interference exhibited by the original analyzer were eliminated. In breath-to-breath measurements in two healthy men, the fractional uptake of O_3 during one minute of quiet breathing was comparable to the results obtained by using a slowly responding commercial analyzer with a quasi-steady material balance method (Wiester et al. 1996). In fact, fractional uptake was about 0.8 regardless of O_3 exposure concentration (0.11 to 0.43 ppm) or ventilation rate (4 to 41 Lpm/m^2).

* A list of abbreviations appears at the end of the Investigators' Report.

This Investigators' Report is one part of Health Effects Institute Research Report Number 79, which also includes a Commentary by the Health Review Committee, and an HEI Statement about the research project. This work improved an ozone analyzer developed earlier by this same group of investigators, as described in HEI Research Reports Numbers 39 and 69. Correspondence concerning the Investigators' Report may be addressed to Dr. James S. Ultman, Pennsylvania State University, Department of Chemical Engineering, 106 Fenske Laboratory, University Park, PA 16802.

Although this document was produced with partial funding by the United States Environmental Protection Agency under Assistance Award R824835 to the Health Effects Institute, it has not been subjected to the Agency's peer and administrative review and therefore may not necessarily reflect the views of the Agency, and no official endorsement by it should be inferred. The contents of this document also have not been reviewed by private party institutions, including those that support the Health Effects Institute; therefore, it may not reflect the views or policies of these parties, and no endorsement by them should be inferred.

INTRODUCTION

People exposed acutely to near-ambient levels of O_3 exhibit decrements in pulmonary function. This has been documented with routine spirometric tests (McDonnell et al. 1983), and biochemical and cellular evidence of tissue inflammation has been found in bronchoalveolar lavage fluid (Koren et al. 1989). The pulmonary function response, in particular, depends on exposure concentration and exercise-induced ventilation rate (Tilton 1989), with considerable variation existing among people (McDonnell et al. 1985). Whereas most investigators have used ambient O_3 concentration alone to characterize exposure conditions, Adams and colleagues (1981) hypothesized that physiological response was more closely related to the product of inhaled concentration, minute ventilation, and exposure time, a quantity they defined as the "effective dose." However, their experiments indicated that this was not strictly true; correlation of decrements in pulmonary function with effective dose alone could not completely account for the effect of exposure concentration. Moreover, this correlation was steeper for women than for men (Lauritzen and Adams 1985), suggesting that other variables such as lung size, tidal volume, or breathing frequency could be important.

The use of effective dose as a surrogate for the actual dose to respiratory tissues does not allow for possible differences in the efficiency of O_3 absorption between individuals or between different breathing patterns in a particular individual. We believe that the uptake of O_3 is a more appropriate dosimeter with which to explain the extent of functional or biochemical response. The determination of this net respiratory dose involves monitoring O_3 concentration at the airway opening using an instrument with a dynamic response that is rapid relative to the respiration frequency. For the extreme case of heavy exercise, the breathing frequency is about 40 breaths per minute (bpm) (Gale et al. 1985). Assuming that the measurement device must respond at 10 times this frequency, its 10% to 90% step-response time should be about 50 msec.

Pearson and Stedman (1980) developed a rapidly responding instrument that used a sample stream containing O_3, which continuously reacted with pure nitric oxide, thereby emitting infrared light. Although the 40-msec re-

sponse time of this chemiluminescent O_3 analyzer would be ideal for respiratory measurements, the toxicity of pure nitric oxide creates a potential hazard for the human subject and for laboratory personnel, making it impractical for routine use. Monitoring O_3 by measuring its gas-phase chemiluminescent reaction with an alkene (Nederbragt et al. 1965) is a much safer basis for a respiratory analyzer. By decreasing the size of both the reaction chamber and the sample inlet tubing of an ethylene-based analyzer originally designed for monitoring environmental O_3 levels, Gerrity and colleagues (1988) were able to reduce response time from 2.2 seconds to 670 msec. Uptake measurements with this analyzer required restricting a subject's breathing frequency to 24 bpm or less, a frequency characteristic of light exercise. Even so, the time-varying O_3 concentration data were not sufficiently accurate to allow exact breath-to-breath calculations of uptake.

Ben-Jebria and associates (1989, 1990) designed a chemiluminescent analyzer that incorporated a needle valve to control the sampling flow, and utilized 2-methyl-2-butene as the reactant gas because it reacts rapidly with O_3. This instrument achieved a response time of 110 msec, which is adequate for respiratory measurements during quiet breathing or light exercise. However, its output signal was influenced by the presence of CO_2 in the air sample, and its calibration became nonlinear below 0.1 ppm O_3. Gerrity and colleagues (1995) eliminated these undesirable performance characteristics by employing ethylene as the reactant gas in an analyzer that was patterned after Ben-Jebria's device in all other respects. This device had a response time of 240 msec, which was suitable for the O_3 uptake measurements that these investigators made during quiet breathing but would not be sufficiently responsive at the higher ventilatory frequencies corresponding to exercise.

In this handful of attempts to develop a safe analyzer to measure O_3 dosimetry in humans, none has achieved a dynamic response that is adequate for measuring breath-to-breath O_3 uptake at the respiration frequencies encountered when people exercise at moderate or heavy levels.

SPECIFIC AIMS

Under a previous HEI research agreement, we developed a fast-responding chemiluminescent O_3 analyzer that is suitable for monitoring O_3 concentration in people who are inhaling and exhaling O_3 at rest or during light exercise (Ultman and Ben-Jebria 1991). To use this device during moderate and heavy exercise, we needed to improve its performance characteristics. During the 16-month period of this research agreement, our specific aims were to build a new O_3 analyzer that would exhibit (1) a decrease in the step-response time from 110 msec to 50 msec, and (2) an increase in the signal-to-noise ratio from 9:1 to 30:1 at 0.1 ppm O_3. In redesigning our original chemiluminescent analyzer to achieve these performance goals, we employed ethylene in place of 2-methyl-2-butene as the reactant gas; we optimized the inlet gas flows and chamber pressure; and we consolidated the analyzer components so they could fit in a small instrument cabinet.

The project was divided into three Phases, each requiring about 5 months to complete. In Phase I, preliminary tests were performed using the original analyzer to determine near-optimal specifications for the improved analyzer. In Phase II, a totally new self-contained analyzer was designed and constructed. In Phase III, this instrument was tuned for optimal performance. We also performed an additional experiment that was not planned in the research proposal. We incorporated the newly constructed analyzer into an inhalation exposure system, and measured the breath-to-breath uptake of O_3 during rest and exercise in two healthy men.

METHODS AND STUDY DESIGN

DESIGN RATIONALE

In our original chemiluminescent analyzer, 0.005 Lpm of pure 2-methyl-2-butene was continuously combined with a 0.400-Lpm sample of respired gas in a 10-mL reaction chamber operated at 200 torr. By detecting the emitted visible light with a photomultiplier tube (PMT) coupled to a high-gain electrometer, a 10% to 90% step-response time of 110 msec was achieved with a minimal detectable O_3 concentration of 0.018 ppm (Ben-Jebria et al. 1990). In developing a new analyzer, the 2-methyl-2-butene was replaced with ethylene to improve the linearity of the calibration as well as to eliminate the influence of CO_2 on the output signal. In a previous comparison of these two alkenes, we found that they produced similar signal-to-noise ratios, but the step-response time for ethylene was five times longer than for 2-methyl-2-butene (Ben-Jebria and Ultman 1989). It should be possible, however, to improve dynamic response by increasing the gas-sampling and ethylene flow rates, particularly during exercise conditions when the rate of respired air flow is relatively rapid.

The original analyzer consisted of five separate components: a reaction chamber coupled to a PMT housing, an electrometer with a self-contained adjustable low-pass filter, a PMT bias voltage supply, a pair of flowmeters to measure gas flows, and a vacuum pump fitted with a vacuum-control valve. In Phase II of this project, we constructed a new instrument in which the reaction chamber,

electrometer, voltage supply, and flowmeters were mounted in a single cabinet (Figure 1; broken lines). In addition to protecting the critical components of the device and enhancing its portability, this physical design had two features aimed at improving analyzer performance. First, we replaced the stand-alone electrometer with one that is integrated into the PMT housing to reduce electronic noise. Second, we installed a ventilation fan in the cabinet, which should improve the thermal stability of the analyzer.

ANALYZER PERFORMANCE TESTS

In testing both the original and the new chemiluminescent analyzers, we relied on two standard performance tests. In the static calibration test, the gas-sampling line was directly connected to a standard ultraviolet O_3 source (Model 49PS, Thermoenvironmental, Franklin, MA), and the analyzer output was recorded in digital form at various O_3 concentrations from 0.02 to 1.0 ppm. The time average of the output, hereafter designated as the "signal" or S, and the root-mean-square of the output, hereafter designated as the "noise" or N, were numerically computed from these digital recordings (Figure 2). A static calibration line was determined by linearly regressing the signal with the corresponding O_3 concentrations. In the test for dynamic step-response time, the air-sampling line was connected to the outlet of a three-way solenoid valve (Series 1, General Valve, Fairfield, NJ) that could rapidly switch its inlet between room air and the ultraviolet O_3 source. The analyzer output then was recorded in digital form as the valve was switched from 0.5 (or 0.1) ppm O_3 in air to room air,

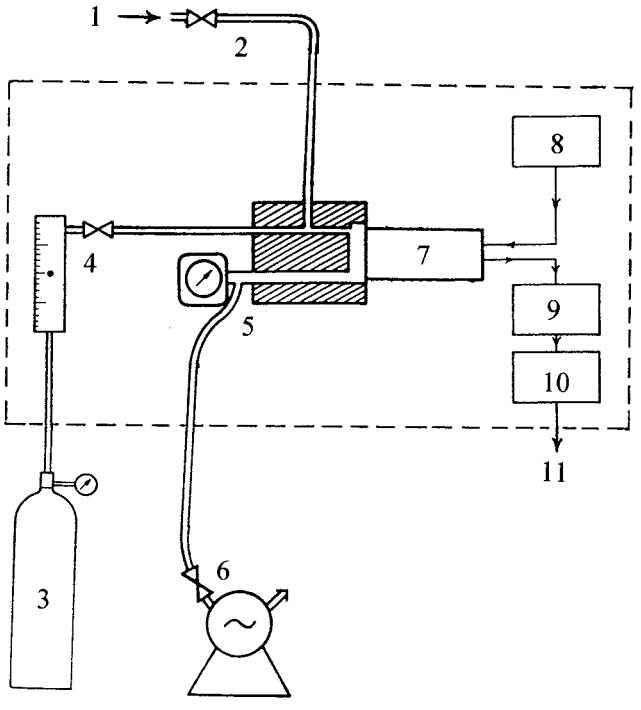

Figure 1. Diagram of the respiratory chemilumescent analyzer. A continuous flow of respired air [1] is admitted into a high-resistance metering valve [2] and travels along a narrow-bore Teflon inlet tube. Pure alkene enters from a pressure-regulated gas cylinder [3] through a flowmeter-valve assembly [4]. The two gas streams mix in a low-volume stainless-steel reaction chamber [5] kept at a constant vacuum by a pump-valve combination [6]. Chemiluminescence is detected by a PMT [7] biased by a high voltage supply [8]. The PMT output current is converted to voltage by an electrometer [9] and then electronically filtered [10] to arrive at the final signal [11]. In the original analyzer, the numbered components were individual, self-contained units. In this analyzer, the electrometer was integrated into the PMT housing, and all the components within the broken lines were mounted in a single metal cabinet.

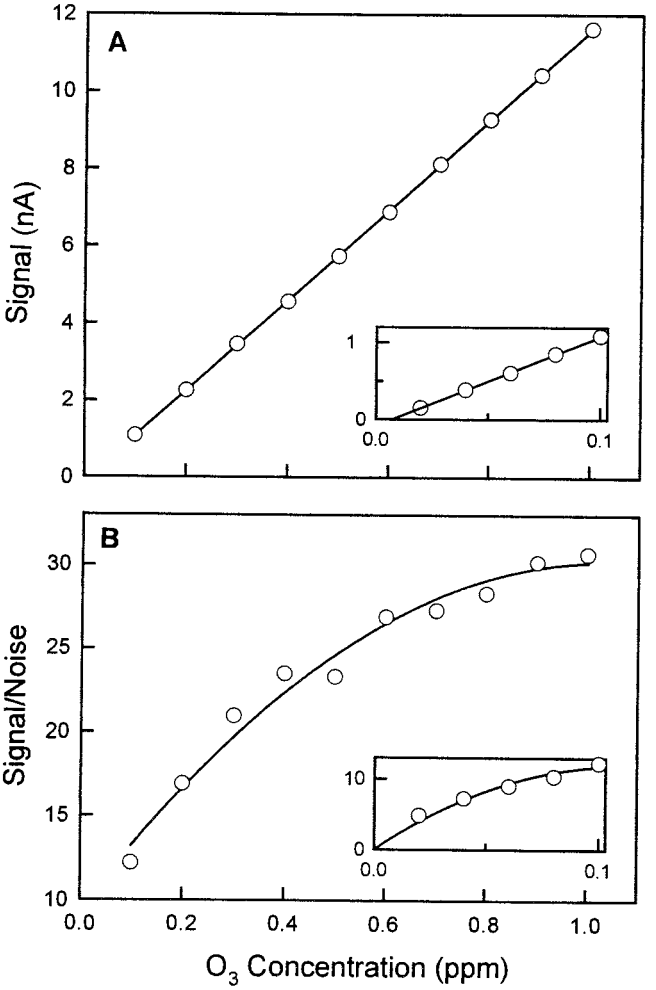

Figure 2. Static calibration test. The signals, electronically filtered at $F = 8$ Hz, were recorded at optimal operating conditions ($P = 350$ torr, $X = 4$, $V_A = 0.6$ Lpm, BV = −800 V) when the sampling line was connected to a source of constant O_3 concentration. (A) The signal was computed as the time average of the PMT current. (B) $S:N$ was computed as the ratio of the signal to the root-mean-square of the current. Each data point results from a single recording of analyzer output.

and then back to 0.5 (or 0.1) ppm O_3 in air (Figure 3). To determine the analyzer response in an objective fashion, a computer code was developed to search the digital recordings for those times when the analyzer output increased by 10% and by 90% from its initial level to its final level.

In both of these performance tests, the analyzer output was digitized at a sampling rate of 200 Hz, and stored on a data acquisition system (570 DAS, Keithly, Taunton, MA). The following performance parameters were routinely computed from the test data:

SEN = sensitivity, the slope of the static calibration line (nA/ppm);

S:N = signal-to-noise ratio, (mean)/(root-mean-square) of the digitized analyzer output; and

RT = response time, time (t) for the stepped output signal to rise from 10% (t_{10}) to 90% (t_{90}) of its final level (msec).

To optimize the value of these performance parameters, three operating parameters and two electronic parameters could be varied:

$\dot{V}_A$ = inlet flow to the analyzer of the respired air sample (Lpm);

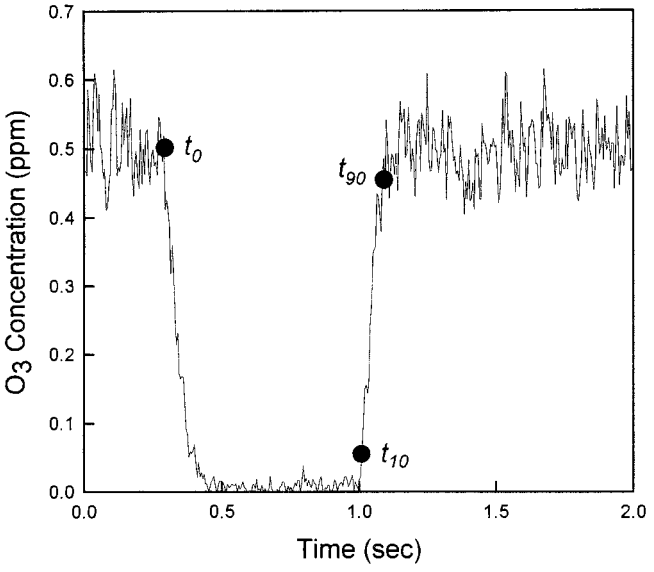

Figure 3. Dynamic performance test. These unfiltered signals were recorded at optimal operating conditions (P = 350 torr, X = 4, $\dot{V}_A$ = 0.6 Lpm, BV = −800 V) when the sampling line was connected to a three-way solenoid valve, which rapidly switched back and forth from 0.5 ppm O_3 to room air. Analyzer transport delay was determined as the time elapsed from switching the valve until the signal first exhibited a decline (t_0 = 295 msec). Response time was measured as the time required for the signal to rise from 10% to 90% of its final steady value ($RT = t_{90} - t_{10}$ = 75.3 msec).

X = ratio of the inlet flow of ethylene to the inlet flow of O_3-containing air sample;

P = absolute pressure in the reaction chamber (torr);

F = cut-off frequency of the low-pass filter (Hz); and

BV = bias voltage of the PMT (V).

In Phase I of the project, we used the original analyzer to confirm that performance could be improved by using ethylene as the reactant gas. First, we modified the analyzer by replacing the 2-methyl-2-butene source with a compressed source of pure ethylene. Then, with the electronic parameters fixed at F = 6 Hz and BV = −700 V, an experimenter varied $\dot{V}_A$ from 0.2 Lpm to 1.0 Lpm, X from 0.8 to 5.2, and P from 160 torr to 440 torr. These variations were conducted in a trial-and-error fashion with the objective of finding a combination of $\dot{V}_A$, X, and P that would give the smallest value of *RT* and the largest value of *S:N*. The best performance, *SEN* = 6.9 nA/ppm, *S:N* = 20:1, and *RT* = 80 msec at 0.5 ppm, occurred at an operating condition of $\dot{V}_A$ = 0.55 Lpm, X = 3.5, and P = 410 torr.

In Phase III of the project, the performance of the new analyzer (constructed in Phase II) was optimized in a series of operating and electronic tests. In all of these tests, the electrometer was set at its maximal gain of 10^8 V/A. Three operating tests were carried out with electronic parameters fixed at BV = −800 V and F→∞ (i.e., unfiltered signal). In the pressure test, $\dot{V}_A$ was set at 0.55 Lpm, X was set at 3.5, and analyzer peformance was evaluated at different P values between 200 and 500 torr. In the flow ratio test, $\dot{V}_A$ was set at 0.6 Lpm, P was set at 350 torr, and performance was evaluated at alternative values for X between 1.0 and 4.5. In the air sample test, X was set at 4, P was set at 350 torr, and performance was evaluated at different levels of $\dot{V}_A$ between 0.2 and 0.8 Lpm.

Two electronic tests were conducted in Phase III with the operating parameters fixed at P = 350 torr, X = 4, and $\dot{V}_A$ = 0.60 Lpm. In the bias voltage test, the unfiltered electrometer output was recorded at BV ranging from −400 to −1000 V. In the filter test, BV was fixed at −800 V and performance was determined when the electrometer output was smoothed with a four-pole low-pass analog filter at alternative F values from 8 to 50 Hz.

Once optimal operating and electronic settings were obtained, the analyzer was tested for CO_2 interference by recording two static calibrations, first with air (i.e., 20% O_2 and 80% nitrogen [N_2]) as the feed gas to the standard O_3 source, and then with a feed gas similar to an exhaled breath (i.e., 5% CO_2, 15% O_2, and 80% N_2). Finally, we evaluated the stability of the analyzer by determining its static calibration every 60 minutes during continuous operation for 6 hours.

HUMAN SUBJECT DEMONSTRATION TEST

To test the new instrument in a typical dosimetry experiment, we continuously monitored the respired flow and O_3 concentration of two healthy nonsmokers (Table 1) in an exposure protocol approved by the Biomedical Committee of the Pennsylvania State University Office for Regulatory Compliance. Each subject alternately breathed 0.11 or 0.43 ppm O_3 while at rest or exercising on a bicycle ergometer (Monarch 850, Quinton Instruments, Seattle, WA) at workloads of 120 or 160 W. For purposes of comparison, 0.12 ppm is the National Ambient Air Quality Standard (NAAQS) enforced by the federal government.

The subjects breathed orally through a mouthpiece assembly that originated from a two-way nonrebreathing valve containing a common port, an inspiratory inlet port, and an expiratory outlet port (2700, Hans Rudolph, Kansas City, MO). The common port was connected to a pneumotachograph (#2, Fleisch, Lausanne, Switzerland) that was fitted at its opposite end with a plastic mouthpiece. The inspiratory port was connected to a 30-L exposure dome containing the desired O_3-air mixture (Asplund et al. 1996), and the expiratory port was exhausted to the room. The sampling line of the O_3 analyzer was connected distally to the pneumotachograph at a distance of 1 cm proximal to the plastic mouthpiece; the differential pressure across the pneumotachograph was detected by an electromagnetic transducer (MP45, Validyne Engineering, Northridge, CA). The voltage signals from both the analyzer and pressure transducer were digitally recorded at 100 Hz by a data acquisition system (DAS1602, Keithly, Tauton, MA) driven by a personal computer (P5-120, Midwest Micro, Fletcher, OH).

Just before an experiment, the pneumotachograph was calibrated with a source of constant air flow, a static calibration of the O_3 analyzer was performed, and the concentration of O_3 in the exposure dome was stabilized at the desired level. While at rest on the bicycle ergometer, the subject breathed the O_3-air mixture through the mouthpiece assembly, and a continuous recording of respiratory flow and O_3 concentration was made for 60 seconds. The subject then pedaled the ergometer at a 120-W workload for 15 minutes, at the end of which a 30-second recording of flow and O_3 concentration was made. The ergometer load was then increased to 160 W and, after 15 more minutes of exercise by the subject, a final 30-second recording of flow and O_3 concentration was made. We repeated this procedure with the individual inhaling O_3 at levels of 0.11 or 0.43 ppm.

Data processing consisted of shifting the O_3 signal to account for the 295 msec transport delay of the analyzer; multiplying the flow and concentration signals by their respective calibration constants; and continously integrating [respired gas flow] × [O_3 concentration] with respect to time to determine O_3 uptake. The calibrated flow signal also was integrated with respect to time to determine the instantaneous respired volume and the minute volume.

Table 1. Characteristics of Tested Human Subjects[a]

Subject	Age (yr)	Height (cm)	Weight (kg)	FVC (L)	FEV_1 (L)	FEV_1/FVC (%)
1	43	163	60	4.3	3.4	79.1
2	50	173	68	5.5	3.7	67.3

[a] FVC = forced vital capacity; and FEV_1 = forced expiratory volume in 1 second

RESULTS

ANALYZER DESIGN

The heart of the new analyzer was the custom-machined reaction chamber (Figures 1 and 4). The 10-mL gas space internal to the chamber was maintained at a constant hypobaric pressure by an external vacuum pump (1004AC, Al-

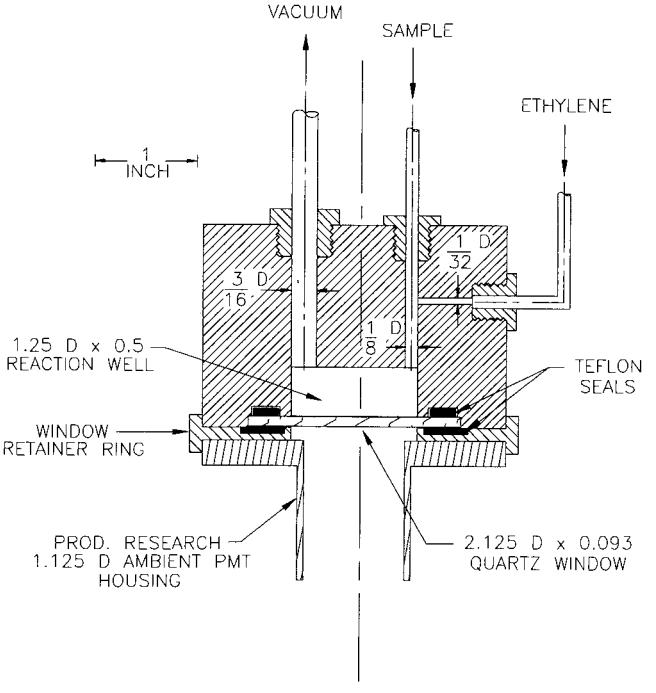

Figure 4. Chemiluminescent reaction chamber. The stainless-steel reaction chamber had an internal volume of 10 mL. The quartz window retaining ring and PMT housing each were fastened to the main steel block by three machine screws (not shown). All dimensions are given in inches. D refers to diameter.

katel, Hingham, MA) fitted with a bellows valve (55-8BW, Nupro, Willoughby, OH). Pure ethylene was supplied at a pressure close to 1 atmosphere (atm) by an L-type gas cylinder fitted with a two-stage pressure regulator. The air sampling stream was drawn through a 135-cm long × 0.32-cm i.d. Teflon tube fitted at its upstream end with a metering valve (S-series Needle Valve, Nupro, Willoughby, OH). The ethylene and air-sampling streams entered the chamber through a mixing tee. By virtue of the small diameter port through which ethylene entered, this gas stream was accelerated and thoroughly mixed with the air stream. Immediately after exiting the mixing tee, the combined gases were swept across the surface of a quartz window (Suprasil, NSG Precision Cells, Farmingdale, NY) through which emitted visible light was detected by a 29-mm-diameter head-on PMT tube (R268, Hamamatsu, Bridgewater, NJ).

With the exception of the sample inlet line, the vacuum pump, and the ethylene source, all components of the analyzer were contained in a cabinet 48 cm × 53 cm × 18 cm (Figure 5). The vacuum pump and ethylene connections and the signal output were located on the rear panel of the cabinet (not shown). The analyzer controls and readouts were accessible on the front panel of the cabinet (Figure 6). The downstream end of the Teflon sampling line was connected to the Sample Port. To check the sampling flow, the air-metering valve at the upstream end of the Teflon sampling line was periodically connected to the Sample rotometer (1-Lpm Visifloat Flowmeter, Dwyer, Michigan City, IN). Ethylene flow was regulated with the Ethylene Adjust valve (S-series Needle Valve, Nupro, Willoughby, OH), and monitored with the Ethylene rotometer (4-Lpm Visifloat Flowmeter, Dwyer, Michigan City, IN). The PMT BV could be regulated continuously from 0 to −1000 V with the Bias Adjust potentiometer and monitored with the PMT Bias digital panel meter (PM452, Nonlinear Systems, San Diego, CA). The Gain switch allowed amplification of the electrometer at 10^5, 10^6, 10^7, or 10^8 V/A, but the gain was set at its maximal value of 10^8 V/A at all times in this study. The Filter switch set the frequency of the analog low-pass filter at 8, 25, or 50 Hz, or the filter could be bypassed (i.e., $F \rightarrow \infty$). The Cell Pressure meter (DP3002-E, Omega Engineering, Stamford, CT) displayed the reaction chamber pressure, and the PMT Output panel meter (F35-1-13-Q, Simpson, Fort Worth, TX) displayed the signal from the analog filter.

The offset control for the electrometer was internal to the PMT enclosure; thus the analyzer cabinet had to be opened to zero the signal. We rejected having a separate buffer amplifier to allow us to zero the electrometer output signal from a front panel control because of the electronic noise it might have generated.

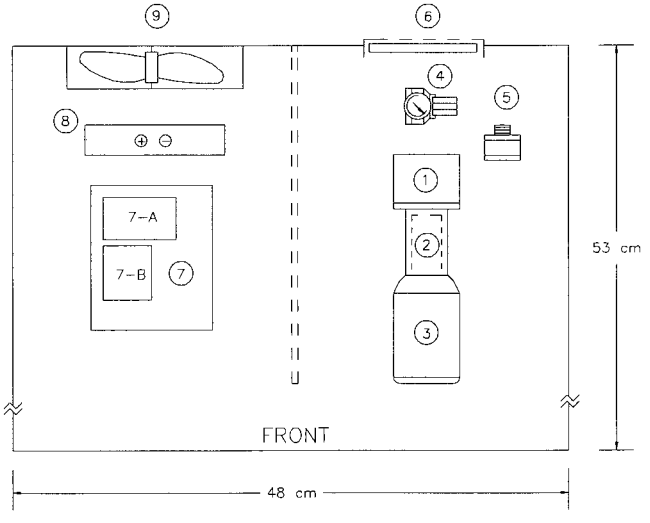

Figure 5. Internal layout of the new analyzer. This top view of the chassis indicates the approximate position and orientation of the major components of the analyzer. [1] Custom-machined reaction chamber; [2] PMT mount and [3] electrometer circuitry integrated into a single enclosure (PR1120RF004, Products for Research, Danvers, MA); [4] low-pressure regulator for ethylene supply (R07-200-RGA, Norgren, Export, PA); [5] absolute pressure transducer for monitoring vacuum in the reaction chamber (PX176-015A5V, Omega Engineering, Stamford, CT); [6] exhaust vent for circulating air; [7] printed circuit electronics board containing [7-A] modular high-voltage supply for biasing the PMT (C1309-06, Hamamatsu, Bridgewater, NJ), and [7-B] four-pole low-pass Butterworth analog filter for smoothing electrometer output (824L8B, Frequency Devices, Haverhill, MA); [8] 5V/12V DC voltage supply for powering electronics (ATV251, Astec, Carlsbad, CA); and [9] AC air fan (MuffinXL, Comair Roton, San Ysidro, CA).

PERFORMANCE DATA

Data from the Phase III operating tests of the newly constructed analyzer are shown in Figures 7, 8, and 9. In the reaction chamber pressure test (Figure 7), values of *S:N* and *RT* both increased as *P* increased, indicating that an improvement in resolution would come at the expense of dynamic response. A pressure of 350 torr gave a reasonable balance between these two performance goals. In the flow

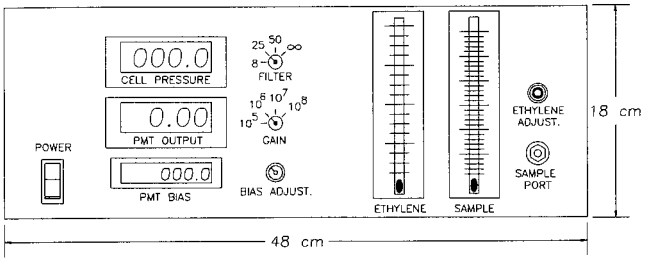

Figure 6. Front panel layout of the new analyzer. The front panel of the instrument included the controls and displays necessary to regulate the ethylene and air-sampling flows, the PMT bias voltage, the electrometer gain, and the analog low-pass filter.

ratio test (Figure 8), *S:N* was virtually constant whereas *RT* decreased with *X*. Because *RT* leveled off at $X = 4$, this became the appropriate value to use for the ethylene:air flow ratio. In the air sample test (Figure 9), *S:N* increased and *RT* decreased with $\dot{V}_A$, indicating that resolution and dynamic response time could both be improved by increasing the inlet air flow. To minimize disturbance of the respired gas stream, however, it was best to limit $\dot{V}_A$ to 0.6 Lpm, the value at which *RT* appeared to level off.

An interesting aspect of these unfiltered performance data is the parallel behavior of *S:N* and *SEN* illustrated by Figure 10. The fact that *S:N* was uniquely correlated with *SEN* independent of *P*, *X*, and $\dot{V}_A$ suggests that noise primarily was due to the PMT and the electrometer rather than to fluidics in the inlet tubing and the reaction chamber. Furthermore, the increase in *S:N* that occurred as *SEN* increased indicates that background interference is an important component of the noise.

The Phase III electronic tests were conducted at the optimal conditions of $P = 350$ torr, $X = 4$, and $\dot{V}_A = 0.6$ Lpm determined in the operating tests. From the PMT bias volt-

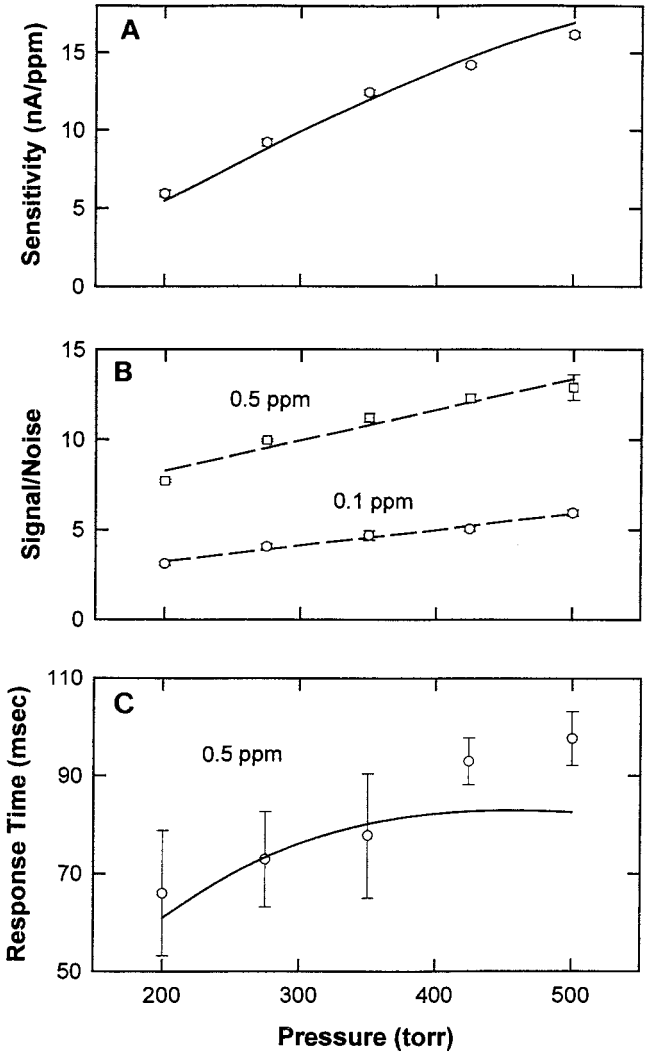

Figure 7. Reaction chamber pressure test. The effect of *P* on performance was determined from the unfiltered signals when $X = 3.5$, $\dot{V}_A = 0.55$ Lpm, and BV = −800 V. Each data point represents the average of five replicate measurements, and the vertical bars indicate the SD around the average (in the absence of bars, the SD is less than the diameter of a data point). The solid curves on the *SEN* (panel A) and *RT* (panel C) plots are the least-squares regression of Equations 1 and 2 to the data points. The interrupted curves on the *S:N* (panel B) plot have no theoretical basis.

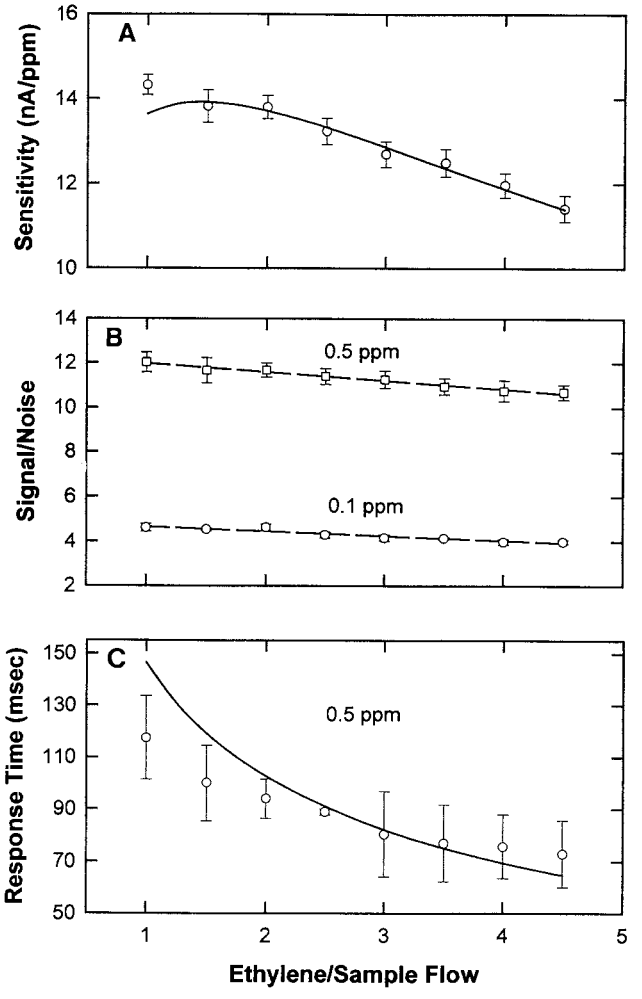

Figure 8. Flow ratio test. The effect of *X* on performance was determined from the unfiltered signals when $\dot{V}_A = 0.6$ Lpm, $P = 350$ torr, and BV = −800 V. Each data point represents the average of five replicate measurements, and the vertical bars indicate the SD around the average (in the absence of bars, the SD is less than the diameter of a data point). The solid curves on the *SEN* (panel A) and *RT* (panel C) plots are the least-squares regression of Equations 1 and 2 to the data points. The interrupted curves on the *S:N* (panel B) plot have no theoretical basis.

age test (Figure 11), it was apparent that instrument resolution was dramatically improved by decreasing BV to a value of −900 V. In practice, BV should be limited to −800 V because of the appearance of high frequency spikes at more negative values (data not shown). In the analog filter test (Figures 12 and 13), both *S:N* and *RT* increased with decreasing *F*, indicating the trade-off between resolution and dynamic response caused by electronic smoothing of the signal. In the continuous monitoring of respired air, in which dynamic response had a higher priority than resolution, analog filtering at 8 Hz was best. In the filter test, a smaller *RT* value was associated with a 0.1-ppm rise in O_3 level than with a 0.5-ppm rise, an unexpected observation that suggested that the dynamic behavior of the analyzer was nonlinear.

The CO_2 interference test was carried out with the operating parameters set at their optimal values. In the absence of CO_2, the slope and intercept of the calibration line were 11.70 ± 0.01 nA/ppm and 0.09126 ± 0.01432 nA, respectively. In the presence of CO_2, the corresponding values were 11.62 ± 0.01 nA/ppm and 0.07359 ± 0.01369 nA. These results suggest that interference from the presence of CO_2 in expired air should be negligible.

The stability test also was conducted at the optimal operating conditions. During the six hours of this test, the temperature varied randomly between 25.2° and 25.6°C. The value of *SEN* also varied randomly from 13.30 to 13.17 nA/ppm, but the intercept of the calibration line varied more systematically from 0.0350 nA at the beginning to 0.0659 nA at the end of the experiment. Therefore, the sensitivity of the instrument was very stable, but the zero reading drifted in six hours by a current equivalent to 0.002 ppm. The correlation coefficients for all seven of the calibration lines in this test were 0.9997 or better, indicating that the linearity of the analyzer was nearly perfect.

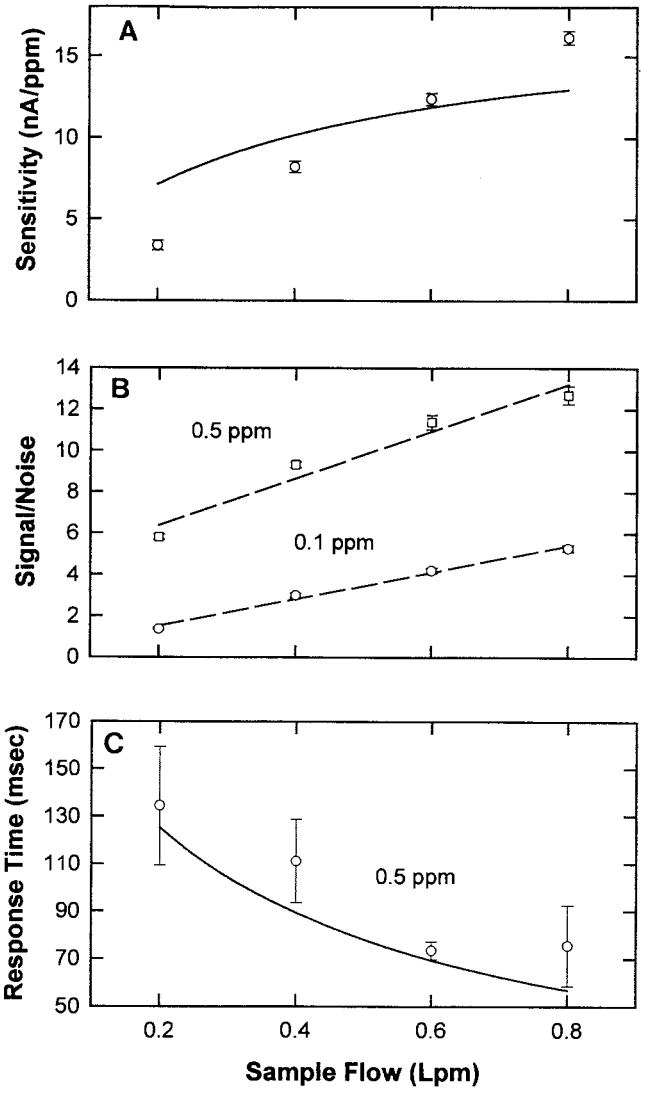

Figure 9. Air sample test. The effect of V_A on performance was determined from the unfiltered signals when $X = 4$, $P = 350$ torr, and BV = −800 V. Each data point represents the average of five replicate measurements, and the vertical bars indicate the SD around the average (in the absence of bars, the SD is less than the diameter of a data point). The solid curves on the *SEN* (panel A) and *RT* (panel C) plots are the least-squares regression of Equations 1 and 2 to the data points. The interrupted curves on the *S:N* (panel B) plot have no theoretical basis.

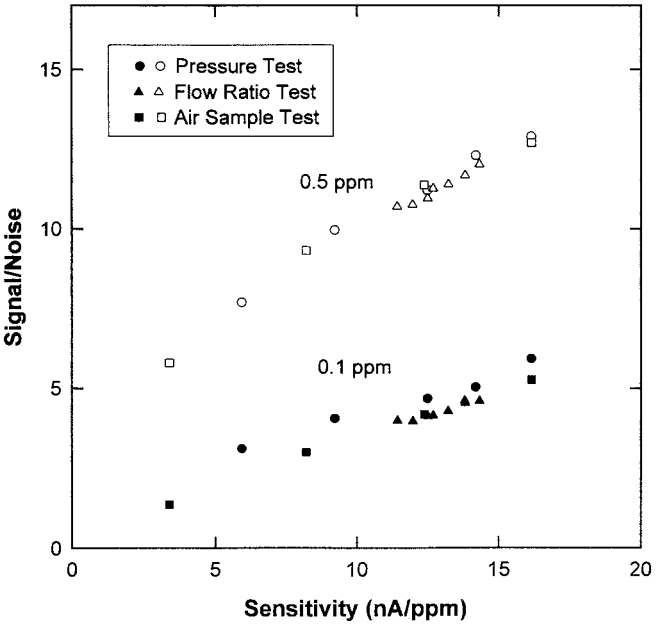

Figure 10. Relationship between *S:N* and *SEN* at 0.1 and 0.5 ppm O_3. This is a cross-plot of the data points from Figures 7, 8, and 9. At a particular O_3 concentration, the relation between *S:N* and *SEN* is independent of the three operating parameters, *P*, *X*, and V_A. This suggests that the noise is primarily electronic in origin.

Table 2 summarizes the optimal performance characteristics and the corresponding operating conditions for both the new and the old analyzers. The dynamic response time, in particular, was improved by increasing the sample flow ($\dot{V}_A$) into the reaction chamber (Figure 9). When increasing $\dot{V}_A$, we wanted to be reasonably certain that respiration would not be disturbed by the sampling process itself. Even at the smallest respired flow expected during quiet breathing, about 12 Lpm, the 0.6-Lpm sampling flow of the new analyzer should be sufficiently small to avoid such a disturbance.

HUMAN SUBJECT DATA

Ozone uptake was measured in two human subjects while at rest and after pedaling a bicycle ergometer at alternate work loads of 120 and 160 W. The 120-W work load elicited ventilation rates from 19 to 24 Lpm/m^2 of body surface area. For the middle-aged men in this study, this was considered to be light-to-moderate exercise. The 160-W work load resulted in ventilation rates from 38 to 41 Lpm/m^2 of body surface area, corresponding to moderate-to-heavy exercise.

Ozone concentration, respired flow, and respired volume signals for a representative series of breaths obtained during a 0.11-ppm-O_3 exposure at 160 W of exercise are shown in Figure 14. Even at this relatively low O_3 concentration and high level of exercise, the noisiness and responsiveness of the O_3 analyzer and pneumotachograph signals were similar. Because the pneumotachograph is an instrument widely accepted for measuring respired flow in exercising subjects, this indicated that the performance of the chemiluminescent analyzer is adequate for its intended application. As

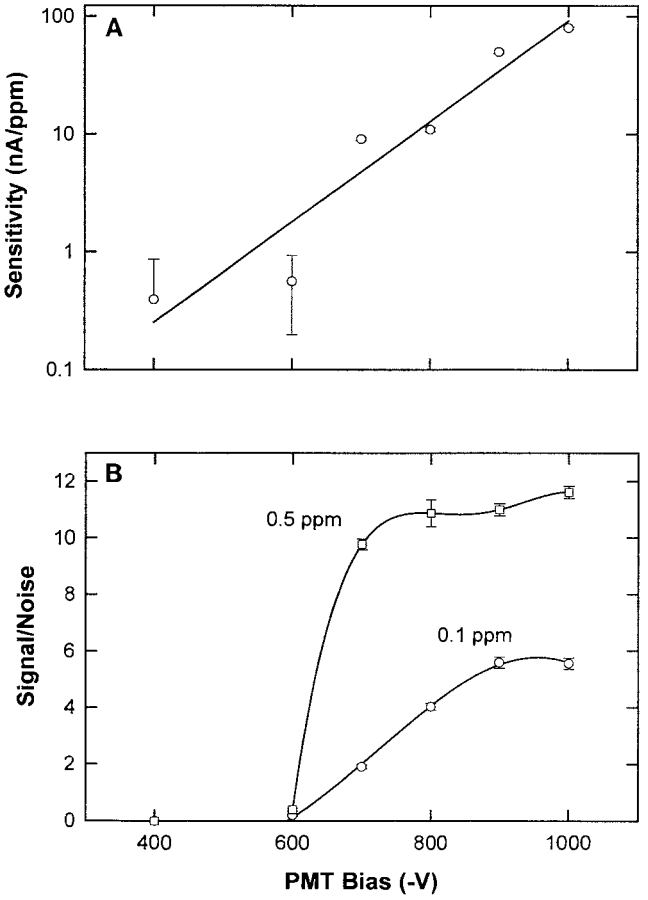

Figure 11. PMT bias voltage test. The effect of BV on performance was determined from the unfiltered signals when $X = 4$, $\dot{V}_A = 0.6$ Lpm, and $P = 350$ torr. Each data point represents the average of five replicate measurements, and the vertical bars indicate the SD around the average (in the absence of bars, the SD is less than the diameter of a data point).

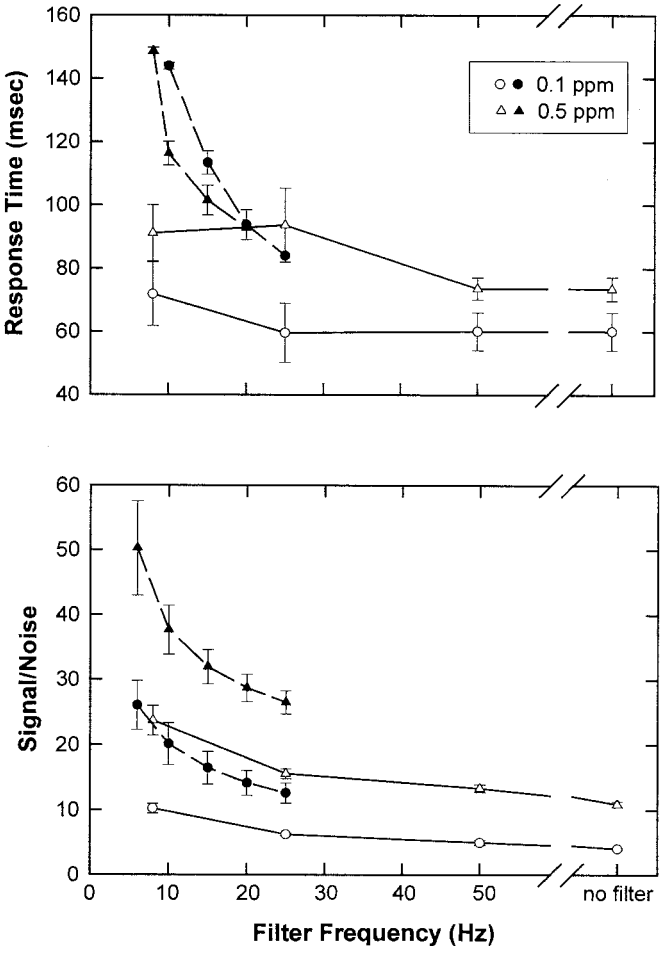

Figure 12. Analog filter test. The effect of F on performance was determined at optimal operating conditions ($P = 350$ torr, $X = 4$, $\dot{V}_A = 0.6$ Lpm, BV = −800 V) for the four-pole analog filter internal to the instrument (unfilled symbols) and for an external eight-pole digital filter (filled symbols). Each data point represents the average of five replicate measurements, and the vertical bars indicate the SD around the average (in the absence of bars, SD is less than the diameter of a data point).

shown in Figure 14, there is a delay of about 150 msec between the respiratory flow reversal (dotted lines) and the sharp inspiratory rise in O_3 concentration. Because the transport delay of the analyzer was taken into account in constructing this figure, the additional 150 msec represents the transport delay through the dead space of the mouthpiece assembly. Judging from the lower graph, the volume of this dead space is about 175 mL, which is consistent with the actual volume of the Hans Rudolf valve and the pneumotachograph.

Figure 15 compares the integrated product of [O_3 concentration] × [respired gas flow] during rest, during 120-W exercise, and during 160-W exercise. With the gas-sampling line located near the subject's lips, this integral represents the cumulative amount of O_3, relative to time zero, that is delivered to the gas space of the lung. Because the time-varying concentration patterns within the gas space are reproducible from breath to breath, the value of the integral at the beginning of any inspiration corresponds to the cumulative uptake of O_3 into respiratory mucosa since time zero. As expected, O_3 uptake is directly affected by the exercise workload.

Each individual breath represented in Figure 15 exhibits a characteristic pattern; a peak value of O_3 uptake is reached during inhalation, followed by a slight decline and then by a plateau during exhalation. The rising portion of a breath corresponds to the cumulative transport of O_3 into the lungs during inhalation. Initially during exhalation, O_3 leaves the conducting airways, leading to a decline in the curve. As

Table 2. Achievement of Performance Goals[a]

	0.1 ppm O_3			0.5 ppm O_3		
	Goal	Old	New	Goal	Old	New
RT (msec)	50	---	70	50	110	90
S:N	30:1	9:1	11:1	--	28:1	24:1

[a] Operating conditions: P = 200 torr, $\dot{V}_A$ = 0.4 Lpm, X = 0.01, F = 6 Hz for the old analyzer; and P = 350 torr, $\dot{V}_A$ = 0.6 Lpm, X = 4, F = 8 Hz for the new analyzer.

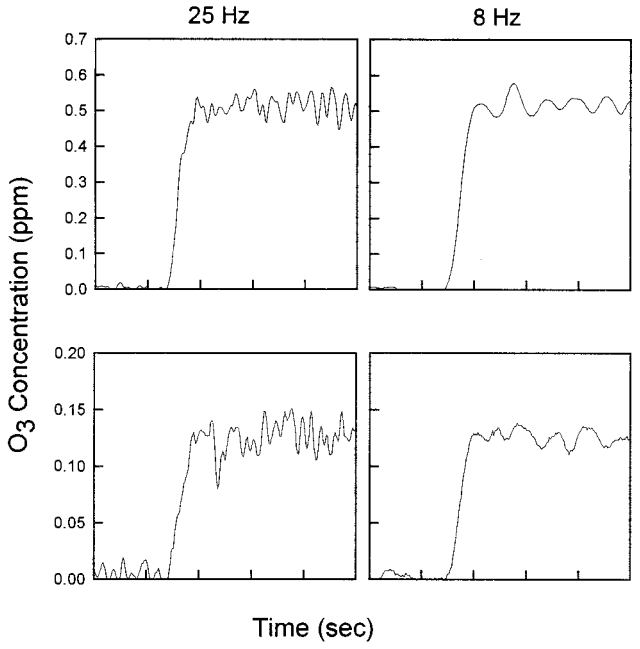

Figure 13. Effect of analog filtering on dynamic signals. These filtered signals were obtained in the dynamic response test at O_3 concentrations of 0.5 ppm (upper panels) and 0.12 ppm (lower panels) when the analyzer was operated at optimal conditions (P = 350 torr, X = 4, $\dot{V}_A$ = 0.6 Lpm, BV = −800 V).

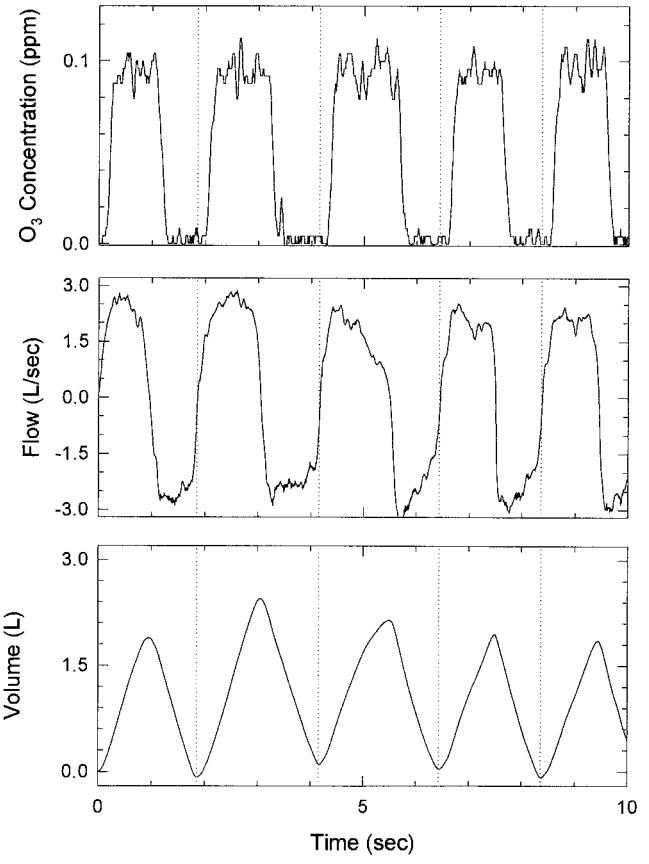

Figure 14. Breath-by-breath data for subject 1. Oral exposure to 0.11 ppm O_3 at an exercise workload of 160 W. The O_3 concentration data have been shifted to correct for the 295 msec transport delay of the analyzer, as determined in the dynamic performance test (Figure 3). The vertical dotted lines correspond to the reversal from exhalation (− respiratory flow) to inhalation (+ respiratory flow).

the anatomical dead space is washed out by alveolar air that is free of O_3, the curve levels off. This pattern in the cumulative uptake curves implies that the fractional uptake of inhaled O_3 during a single breath was less than 1.0.

Table 3 summarizes both the uptake rate and the fractional uptake per breath. Uptake rate was obtained by dividing the cumulative uptake obtained from a series of 12 to 15 breaths by the corresponding time period. Fractional uptake was obtained by determining the integral of [O_3 concentration] × [respired gas flow] separately during the inspiratory and expiratory phases of the breaths. As expected, the uptake rate increased with minute volume and exposure concentration, as well as exercise level. However, for the two subjects tested, there appeared to be no systematic variation in fractional uptake with ventilation rate or with exposure concentration.

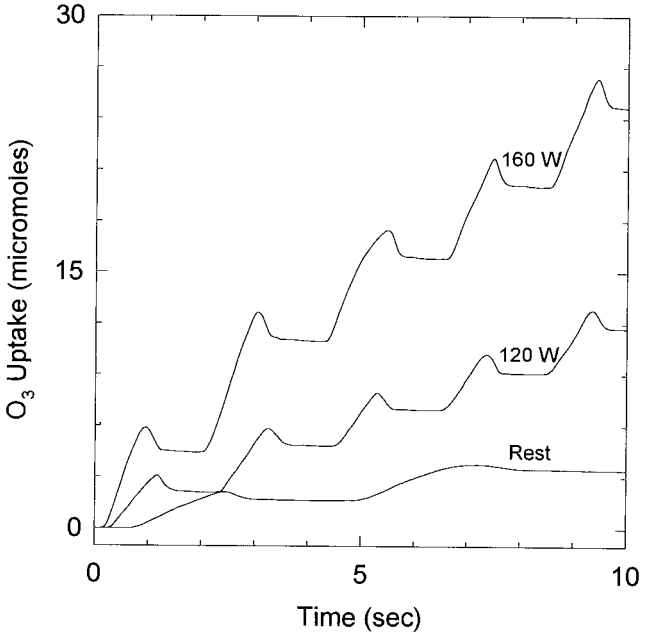

Figure 15. Continuous uptake for subject 1 during oral exposure to 0.11 ppm O_3. Uptake was determined as the running integration of [O_3 concentration] × [respired gas flow] with respect to time.

DISCUSSION

ANALYZER PERFORMANCE

In the chemiluminescent respiratory O_3 analyzer (Figure 1), an ozone-containing air sample [1-2] is continuously mixed with a stoichiometric excess of pure ethylene [3-4] in a reaction chamber [5] maintained at a constant hypobaric pressure by a vacuum pump [6]. When O_3 and ethylene combine, they form a high-energy intermediate that emits light during its spontaneous transformation into a stable aldehyde. This chemiluminescent process is partially quenched by diluent gas molecules such as nitrogen and oxygen that compete for reaction with the intermediate. Because the O_3-ethylene luminescence has a wavelength of 300 to 600 nm, it can be continuously detected by a PMT having broad spectral sensitivity to visible light [7-11].

Performance tests were carried out to maximize dynamic response time and resolution by manipulating reaction chamber pressure, P; the ethylene to sample flow ratio, X; and sample flow, V_A. As an aid for interpreting results, we developed a mathematical model (Appendix A) similar to the one published by Mehrabzadeh and colleagues (1983). The key assumption in the model is that the gas in the

Table 3. Ventilation and Uptake Parameters in Human Subject Experiments

		Ventilation Rate (Lpm)		Frequency (bpm)		O_3 Uptake (nmol/min)		Fractional Uptake	
O_3 (ppm)	Workload (W)	Subject 1	Subject 2	Subject 1	Subject 2	Subject 1	Subject 2	Subject 1	Subject 2
0.11	0	8.3	7.4	12.7	11.8	15.2	12.4	0.76	0.80
	120	35.4	35.0	31.0	26.1	67.9	71.1	0.67	0.78
	160	63.7	74.5	31.7	36.4	148.0	164.2	0.75	0.78
0.43	0	9.0	9.4	13.5	17.0	75.6	61.8	0.81	0.69
	120	39.1	34.2	25.7	27.4	375.4	316.2	0.77	0.77
	160	61.5	72.2	32.5	33.8	625.6	758.4	0.76	0.79

reaction chamber is perfectly mixed. It follows from model Equations A10 and A11 that the 10% to 90% response time is given by:

$$RT = 2.20\,[k_1C(P/P_i)X/(1+X) + (1+X)(\dot{V}_A/V)(P_i/P)]^{-1} \quad (1)$$

where k_1 is the rate constant of the O_3-ethylene reaction, C is the molar gas density at the atmospheric inlet pressure, P_i, and V is the reaction chamber volume. A nonlinear regression of RT data (Figures 7, 8, and 9) to Equation 1 was performed by using a nonlinear optimization algorithm (Excel 5.0 Solver, Microsoft Corp.) for minimizing the summed square error. The results were not satisfactory when k_1 was employed as the only adjustable parameter. When V and k_1 were treated as adjustable parameters, however, a reasonable regression was obtained (Figures 7, 8, and 9; continuous curves). The best estimate of $V = 5.13$ mL was smaller than the actual reaction chamber volume of 10 mL. This probably was due to stagnation regions, peripheral to the main sweep flow in the reaction chamber, that did not substantially contribute to chemiluminescence. The best estimate of $k_1 = 1.17 \times 10^{-18}$ mL/molec-sec was similar to the value of 1.9×10^{-18} mL/molec-sec previously reported (Japar et al. 1974).

Equation 1 indicates that RT is inversely proportional to the sum of $k_1C(P/P_i)X/(1+X)$, the characteristic O_3 reaction rate, plus $(1+X)(\dot{V}_A/V)(P_i/P)$, the characteristic gas transit rate through the reaction chamber. The decrease in the RT measurements observed when X increased (Figure 8) resulted from an increase in reaction rate as well as transit rate, but the decrease in RT associated with an increase in $\dot{V}_A$ (Figure 9) only could have resulted from an increase in the transit rate. The increase in RT prompted by an increase in P (Figure 7) demonstrates that the transit rate had a stronger influence on RT than did the reaction rate.

The sensitivity of the analyzer can be predicted from model Equation A10 as I:C_{Oi}, which is the ratio of [the intensity of emitted light per unit volume of reacting gas (I)] to [the molar O_3 concentration at the analyzer inlet (C_{Oi})] reached at steady state (i.e., very large values of t).

$$SEN = [(\kappa\dot{V}_A RT/2.20)(k_1CXP/P_i)/(1+X)] \times [1 + (k_2CP/P_i)/(1+X)]^{-1} \quad (2)$$

where k_2 is a quenching constant, and κ is a proportionality constant that accounts for the transduction of light intensity into an electrical output current. A nonlinear least-squares regression of SEN data to Equation 2 gave reasonable results (Figures 7, 8, and 9) when κ and k_2 were treated as adjustable parameters whose best estimates were 3.96 nA-sec/ppm-mL and 4.77×10^{-20} mL/molec, respectively. Because the quenched fraction of high-energy intermediate, $(k_2CP/P_i)/(1+X)$, usually was much less than 1.0 for the operating conditions employed in the experiments, the analyzer sensitivity was determined primarily by the variables in the numerator of Equation 2, $RT \bullet \dot{V}_APX/(1+X)$. For example, when P was increased, RT also increased so that SEN increased (Figure 7). On the other hand, as X increased, the decrease in RT was sufficiently sharp that SEN also declined, even though $X/(1+X)$ increased (Figure 8). Finally, as $\dot{V}_A$ increased, the corresponding decrease in RT was sufficiently small that SEN increased (Figure 9).

In addition to correlating performance data, the mathematical model can suggest further improvements in analyzer design or operation. For example, the reaction chamber volume was not varied in this study, but it is apparent from Equation 1 that decreasing V could have the desirable effect of reducing RT. Judging from Equation 2, a reduction in RT would also diminish SEN and, according to the data in Figure 10, this would diminish S:N. To illustrate this trade-off between improved RT but compromised S:N, suppose the "effective" volume of the present reaction chamber was halved. In that case, the model predicts that RT would decrease from 69.5 msec to 41.6 msec, and SEN would simultaneously decrease from 11.9 to 7.2 nA/ppm. This drop in SEN would cause a decrease in S:N from 11:1 to 8:5 at 0.5 ppm O_3 and from 4:1 to 2:1 at 0.1 ppm O_3. Therefore, unless noise also could be reduced, it would not be desirable to decrease the reaction chamber volume.

Low-pass electronic filtering can attenuate noise; provided that the noise is of sufficiently high frequency, the adverse effect on dynamic response time is minor. For example, analog filtering at 8 Hz almost tripled S:N at 0.1 ppm O_3, from 4:1 to 11:1, while causing a small increase in RT from 60 to 70 msec (Figure 12; unfilled symbols). In an attempt to increase S:N closer to the goal of 30:1 at 0.1 ppm, an additional filtering test was conducted; the analog filter internal to the instrument was set at $F = 50$ Hz, and the resulting signal was further smoothed by an external low-pass digital filter (ASYST Software Technologies, Rochester, NY). The sharp cutoff characteristics of the digital filter dramatically increased S:N, coming close to the 30:1 goal at $F = 8$ Hz, but it also increased RT to a value of 150 msec (Figure 12, filled symbols). Analog filtering is preferable, therefore, in the intended application of the analyzer.

The residual noise in the filtered signal exhibited a surprisingly regular periodicity (Figure 13). The occurrence of this low-frequency noise, probably inherent in the operation of the electrometer, is the limiting factor in the S:N that can be achieved at low O_3 concentrations (inset to lower panel of Figure 2). In particular, the O_3 level at which S:N = 1:1, one representation of the minimal detectable concentration of the analyzer, was 0.006 ppm when the signal was

filtered at 8 Hz. Alternatively, with the specification that $S:N = 2:1$, the minimal detectable concentration was 0.012 ppm.

MEASUREMENTS ON HUMAN SUBJECTS

Only a few measurements of O_3 uptake during continuous exposure have been reported previously. Gerrity and colleagues (1988) monitored O_3 concentration in the posterior pharynx of 18 healthy men using a nasopharyngeal sampling tube connected to an ethylene-based chemiluminescent analyzer with a 10% to 90% step-response time of 670 msec. While at rest, the subjects breathed O_3 concentrations of 0.1, 0.2, and 0.4 ppm at ventilation rates of 10 and 19 Lpm. From these measurements, those investigators computed regional uptake into the extrathoracic airways during inhalation and into the intrathoracic airways during a complete respiratory cycle. To compensate for their analyzer's slow response time, their computations were based on the maximal and minimal O_3 levels of the single-breath concentration curves. To compare our data with theirs, we assumed that their values for fractional uptake into the extrathoracic airways during inhalation would be the same during exhalation, and then estimated fractional uptake in the entire respiratory system from their regional uptake values. The resulting value of 0.96 for fractional uptake was insensitive to ventilation rate and to exposure concentration.

Using a similar pharyngeal sampling tube connected to the same analyzer, Gerrity and associates (1994) determined extrathoracic and intrathoracic O_3 uptake in 20 healthy men. While exercising on a treadmill, they breathed at an oral ventilation rate of 20 Lpm/m^2 of body surface area and continuously inhaled 0.4 ppm O_3. Improvements in that study included the incorporation of continuous flow data in the computation of regional uptake, and the use of a dynamic correction algorithm to compensate partially for the 1.2-sec step-response time of the analyzer. On the basis of their regional uptake values, we estimated the fractional uptake for the entire respiratory system to be 0.88. Employing an ethylene-based analyzer similar in design to that of Ben-Jebria and coworkers (1990), Gerrity and coworkers (1995) continuously measured oral as well as bronchial concentrations of O_3 in 10 adults during quiet breathing of 0.4 ppm O_3 at a ventilation rate of about 9 Lpm. After they employed a dynamic correction for the 250-msec step-response time of the analyzer, their data indicated that fractional uptake for the entire respiratory system was 0.91. Therefore, the latter two studies by Gerrity and colleagues consistently demonstrate that fractional uptake is about 0.9. This is 10% to 15% greater than the values we determined in our demonstration experiments.

Wiester and coworkers (1996) measured average O_3 uptake into the lungs of 10 healthy men who breathed quietly from a mask affixed to a large-diameter pipe through which 0.3 ppm ozonated air was flowing. They determined fractional uptake by measuring the upstream-to-downstream drop in the quasi-steady O_3 concentration in the pipe thereby avoiding the need for a fast-responding instrument. However, this breathing circuit would be too cumbersome to use during exercise. These investigators reported a fractional uptake range from 0.51 to 0.96, with a mean of 0.75, during oral breathing at a ventilation rate of 10 Lpm. This mean value lies between the values of 0.81 and 0.69 measured for the two subjects in the current study during quiet breathing and 0.43 ppm O_3 exposure.

The observation from the demonstration data (Table 3) that fractional uptake was insensitive to exposure concentration implies that the underlying diffusion and chemical reaction processes are linear. This would be the case, for example, if O_3 diffusion followed Fick's Law and biochemical substrates were in sufficient excess that O_3 reacted with tissue by first-order kinetics. The additional observation that fractional uptake does not vary systematically with respiratory flow can be explained on the basis of previous O_3 bolus inhalation experiments conducted in our laboratory (Hu et al. 1992). In particular, an increase in respiratory flow results in a distal shift in the absorption distribution, implying that less O_3 is removed by conducting airway tissue. During exercise, however, tidal volume as well as respiratory flow becomes greater. Therefore, a larger proportion of the inhaled breath reaches the respiratory airspaces, where O_3 absorption is almost 100% efficient. If diminished conducting airway absorption was balanced by increased uptake in the respiratory zone, overall uptake fraction would be independent of flow.

SUMMARY

In this study, we used the basic design of our original methyl-butene–based chemiluminescent analyzer (Ben-Jebria et al. 1990) in a more self-contained ethylene-based instrument. Table 2 compares the specific goals of this study with the performance of both the new and the old analyzer. Note that (1) the minimal detectable O_3 concentration (evaluated at $S:N = 1:1$) of 0.018 ppm achieved with the old analyzer was improved to 0.006 ppm in the new instrument; (2) the static calibration of the old device was nonlinear below 0.1 ppm O_3, but was completely linear for the new analyzer; and (3) the old analyzer was subject to interference by carbon dioxide, whereas the new instrument was not.

The improvement in analyzer performance to RT = 70 msec and $S{:}N$ = 11:1 at 0.1 ppm fell short of the desired specifications of RT = 50 msec and $S{:}N$ = 30:1 at 0.1 ppm. This restricts the device to a maximal breathing frequency of 30 bpm (moderate-to-heavy exercise conditions) at a minimal exposure concentration of 0.1 ppm. Because the NAAQS is currently 0.12 ppm O_3, this limit encompasses most situations in which people are normally exposed to O_3 outdoors. At lower breathing frequencies, at which a longer response time can be tolerated, the resolution of the instrument can be improved by more agressive low-pass filtering of the signal. Conversely, at higher exposure concentrations, in which less absolute resolution is necessary, it is possible to improve dynamic response by less agressive filtering.

In demonstration measurements of total respiratory O_3 absorption in two healthy men, the fractional uptake during quiet breathing was comparable to the results obtained with a commercially available analyzer in a quasi-steady material balance method (Wiester et al. 1996). In fact, fractional uptake was about 0.8 regardless of O_3 exposure concentration (0.11 to 0.43 ppm) or ventilation rate (4 to 41 Lpm/m^2).

ACKNOWLEDGMENTS

Mr. Carl Volz, Jr. provided valuable assistance in the electronic design, and Mr. Thomas R. Gervais was responsible for regressing the performance data to the mathematical model.

REFERENCES

Adams WC, Savin WM, Christo AE. 1981. Detection of ozone toxicity during continuous exercise via the effective dose concept. J Appl Physiol 51:415–422.

Aimedieu P, Barat J. 1981. Instrument to measure stratospheric ozone with high resolution. Rev Sci Instrum 52:432–427.

Asplund PT, Ben-Jebria A, Ultman JS. 1996. A portable inhalation system for personal exposure to ozone. Arch Environ Health 51:138–145.

Ben-Jebria A, Hu S-C, Ultman JS. 1990. Improvements in a chemiluminescent analyzer for respiratory applications. Rev Sci Instrum 61:3435–3439.

Ben-Jebria A, Ultman JS. 1989. Fast-responding chemiluminescent ozone analyzer for respiratory applications. Rev Sci Instrum 60:3004–3011.

Gale GE, Torre-Bueno JR, Moon RE, Saltzman HA, Wagner PD. 1985. Ventilation-perfusion inequality in normal humans during exercise at sea level and simulated altitude. J Appl Physiol 58:978–988.

Gerrity TR, Biscardi F, Strong A, Garlington AR, Brown JS, Bromberg PA. 1995. Bronchoscopic determination of ozone uptake in humans. J Appl Physiol 79:852–860.

Gerrity TR, McDonnell WF, House DE. 1994. The relationship between delivered ozone dose and functional responses in humans. Toxicol Appl Pharmacol 124:275–283.

Gerrity TR, Weaver RA, Berntsen J, House DE, O'Neil JJ. 1988. Extrathoracic and intrathoracic removal of O_3 in tidal-breathing humans. J Appl Physiol 65:393–400.

Hu SC, Ben-Jebria A, Ultman JS. 1992. Longitudinal distribution of ozone absorption in the lung: Effects of respiratory flow. J Appl Physiol 73:1655–1667.

Japar SM, Wu CH, Niki H. 1974. Rate constants for the reaction of ozone with olefins in the gas phase. J Phys Chem 78:2318–2320.

Koren HS, Devlin RB, Graham DE, Mann R, McGee MP, Horstman DH, Kozumbo WJ, Becker S, House DE, McDonnell WF, Bromberg PA. 1989. Ozone-induced inflammation in the lower airways of human subjects. Am Rev Respir Dis 139:407–415.

Lauritzen SK, Adams WC. 1985. Ozone inhalation effects consequent to continuous exercise in females: Comparison to males. J Appl Physiol 59:1601–1606.

McDonnell WF, Horstman DH, Hazucha MJ, Seal E, Haak ED, Salaam SA, House DE. 1983. Pulmonary effects of ozone exposure during exercise: Dose-response characteristics. J Appl Physiol 54:1345–1352.

McDonnell WF, Horstman DH, Abdul-Salaam S, House DE. 1985. Reproducibility of individual responses to ozone exposure. Am Rev Respir Dis 131:36–40.

Mehrabzadeh AA, O'Brien RJ, Hard TM. 1983. Generalized response of chemiluminescence analyzers. Rev Sci Instrum 54:1712–1718.

Nederbragt GW, van der Horst A, van Duijn J. 1965. Rapid ozone determination near an accelerator. Nature 206:87.

Pearson R, Stedman DH. 1980. Instrumentation for fast-response ozone measurements from aircraft. Atmos Technol 12:51–54.

Tilton BE. 1989. Health effects of tropospheric ozone. Environ Sci Technol 23:257–263.

Ultman JS, Ben-Jebria A. 1991. Noninvasive Determination of Respiratory Ozone Absorption: Development of a Fast-Responding Ozone Analyzer. Research Report Number 39. Health Effects Institute, Cambridge, MA.

Wiester M J, Stevens MA, Menche MG, McKee JL, Gerrity TR. 1996. Ozone uptake in healthy adult males during quiet breathing. Fundam Appl Toxicol 29:102–109.

APPENDIX A. Perfectly Mixed Reactor Model of Analyzer Performance

Aimedieu and Barat (1981) described the gas-phase reaction kinetics between O_3 and ethylene in which light is produced by the spontaneous decomposition of a high-energy intermediate; quenching occurs simultaneously by the competitive reaction of the intermediate with diluent molecules such as oxygen and nitrogen. According to these kinetics, the molar rate of O_3 conversion to intermediate per unit volume of reacting gas is given by:

$$r_O = k_1 C_O C_E \quad \text{(A1)}$$

where k_1 is a reaction rate constant, and C_O and C_E are the molar concentrations of O_3 and ethylene, respectively. Moreover, the intensity of the emitted light per unit volume of reacting gas is:

$$I = [k_1/(1+k_2 C_M)] C_O C_E \quad \text{(A2)}$$

where C_M is the molar concentration of the diluent molecules, and $k_2 C_M$ is the fraction of the high-energy intermediates that are quenched without emitting light.

In our O_3 analyzer (Figure 1), a sampling stream consisting of practically pure diluent gas and a low concentration of O_3 is mixed with a pure ethylene stream. Initially, both streams are very close to ambient pressure but, after being drawn through two metering valves by a vacuum pump, their pressure becomes subatmospheric and their volumetric flow rates increase. Assuming an isothermal gas expansion across the metering valves from an atmospheric inlet pressure, P_i, to a hypobaric downstream pressure, P, and also assuming that the molar gas densitites of ethylene and sampled air are equal at the inlet to the analyzer, then the mixed gas stream entering the reaction chamber will have a volumetric flow of:

$$\dot{V} = (P_i/P)(1+X)\dot{V}_A \quad \text{(A3)}$$

a molar O_3 concentration of:

$$C_O' = C_{Oi}(P/P_i)/(1+X) \quad \text{(A4)}$$

a molar ethylene concentration of:

$$C_E = C(P/P_i)/(1+X) \quad \text{(A5)}$$

and a molar diluent concentration of:

$$C_M = C(P/P_i)X/(1+X) \quad \text{(A6)}$$

where $\dot{V}_A$ is the sampling stream flow, X is the ratio of ethylene to sampling stream flow, C_{Oi} is the molar O_3 concentration, and C is the molar gas density, all evaluated at the analyzer inlet.

Within the reaction chamber, the concentrations of ethylene and diluent gas are essentially constant, but O_3 is depleted at a rate that is equal to its output rate less its input rate plus its disappearance by chemical reaction. Assuming that the reaction chamber is perfectly mixed, this can be expressed by:

$$V(-dC_O/dt) = \dot{V}C_O - \dot{V}C_O' + Vr_O \quad \text{(A7)}$$

where V is the volume of the reaction chamber, C_O is the molar O_3 concentration exiting the chamber, and t is time. In the test for step-response time of analyzer dynamics, C_O is initially zero and C_O' is rapidly stepped up from zero to a constant value. In that case, Equation A7 can be combined with Equation A1 and then integrated to find the O_3 response :

$$C_O = C_O' [1 - \exp(-t/\tau)] \quad \text{(A8)}$$

where

$$\tau = (k_1 C_E + \dot{V}/V)^{-1}. \quad \text{(A9)}$$

The predicted change in light intensity resulting from this test for step-response time is found by substituting Equations A3 through A6 into Equations A8 and A9 such that:

$$I = [(\dot{V}_A RT/2.20)(k_1 CXP/P_i)/(1+X)] \times [1 + (k_2 CP/P_i)/(1+X)]^{-1} [1 - \exp(-t/\tau)] C_{Oi} \quad \text{(A10)}$$

and

$$\tau = [k_1 C(P/P_i)X/(1+X) + (1+X)(\dot{V}_A/V)(P_i/P)]^{-1}. \quad \text{(A11)}$$

ABOUT THE AUTHORS

James S. Ultman is a Professor of Chemical Engineering at the Pennsylvania State University, where he has been a faculty member since 1970. He received his Ph.D. in chemical engineering at the University of Delaware in 1969, and then served as a National Institutes of Health Postdoctoral Fellow at the University of Minnesota. In 1978, Professor Ultman was a Fulbright Lecturer at the Technion (Israel Institute of Technology), and a visiting researcher at the Silverberg Medical School (Haifa, Israel). In 1989, he was a Visiting Research Professor in the Department of Medicine of Duke University Medical School. Dr. Ultman is interested in the application of the physical principles of fluid flow, diffusion, and chemical reaction to problems in pulmonary physiology, pathology, and toxicology.

Abdellaziz Ben-Jebria was a Research Scientist at the Institut National de la Santé et de la Recherche Médicale (INSERM, France), working in the Respiratory Pathophysiology Re-

search Unit in Paris from 1980 to 1984, and thereafter in the Physiology Laboratory at the University of Bordeaux-II. Dr. Ben-Jebria earned a Ph.D. in biophysics in 1979 and a State Doctorate degree in natural science in 1984, both at the University of Pierre and Marie Curie in Paris. From 1987 to 1990, he was a Visiting Associate Professor in the Department of Chemical Engineering at the Pennsylvania State University where he is now an Associate Professor. His major research interests are pulmonary gas transport and uptake processes as well as airway reactivity in toxicology.

Craig S. Mac Dougall is a process engineer at the Colgate-Palmolive Company. He served as a military paramedic in the US Army, and then pursued his Bachelor's degree in Chemical Engineering at Pennsylvania State University, graduating in 1996.

Marc L. Rigas is an environmental scientist at the National Exposure Research Laboratory of the US Environmental Protection Agency. He received a bioengineering education at the University of Pennsylvania (B.S.-1992) and Pennsylvania State University (M.S.-1994 and Ph.D.-1997). His research interests are in computer modeling, toxicant dosimetry and risk assessment.

PUBLICATIONS RESULTING FROM THIS RESEARCH

Mac Dougal CS, Rigas ML, Ben-Jebria A, Ultman JS. 1997. A respiratory ozone analyzer optimized for high resolution and swift dynamic response during exercise conditions. Arch Environ Health (in press).

ABBREVIATIONS

atm	atmosphere
bpm	breaths per minute
BV	bias voltage of the photomultiplier tube (always a negative value)
C	molar gas density at analyzer inlet
C_E	molar concentration of ethylene in the reaction chamber
C_M	molar concentration of diluent molecules in the reaction chamber
C_O	molar concentration of O_3 exiting the reaction chamber
$C_{O'}$	molar concentration of O_3 entering the reaction chamber
C_{Oi}	molar concentration of O_3 at the analyzer inlet
CO_2	carbon dioxide
F	cutoff frequency of the low-pass filter
$F \rightarrow \infty$	unfiltered signal
FEV_1	forced expiratory volume in 1 second
FVC	forced vital capacity
I	intensity of emitted light per unit volume of reacting gas
κ	proportionality constant
k_1	rate constant of the O_3-ethylene reaction
k_2	quenching constant of the O_3-ethylene reaction
Lpm	liters per minute
molec	molecules
N	noise
N_2	nitrogen
NAAQS	National Ambient Air Quality Standard
O_2	oxygen
O_3	ozone
P	absolute pressure in the reaction chamber
P_i	absolute pressure at the analyzer inlet
PMT	photomultiplier tube
ppm	concentration of O_3 in parts per million
r_O	molar rate of O_3 conversion per unit volume of reacting gas
RT	response time
S	signal
SEN	sensitivity (slope of the static calibration line)
$S{:}N$	signal-to-noise ratio
τ	exponential time constant
t	time
t_{10}, t_{90}	time for output signal to increase to 10% or 90% of its final level
V	reaction chamber volume
$\dot{V}_A$	inlet flow to analyzer of respired air sample
$\dot{V}$	total mixed gas flow entering reaction chamber
X	ratio of inlet flow of ethylene to the inlet flow of O_3-containing air sample

INTRODUCTION

In humans, exposure to ozone, an irritant gas and ubiquitous air pollutant, has been associated with reversible decreases in certain measures of lung function, increases in airway reactivity, and the appearance of indicators of respiratory tract inflammation in lung lavage fluid. Animal studies indicate that a major site of ozone-related injury is the bronchiole entrance to the acinus of the lung. Human studies suggest a high degree of interindividual variability in respiratory response to ozone exposure as a result of either differential tissue sensitivity or variable delivery of ozone to sensitive tissues. Individuals at increased risk of developing adverse effects following short-term exposures to ozone include those who exercise or engage in moderate-to-strenuous physical activity (reviewed by Lippmann 1989, 1993; Bates 1995; U.S. Environmental Protection Agency 1996).

In order to estimate the health risk that ozone exposure may pose to humans, regulators need to know how ozone exposure, dose to the respiratory tract, and subsequent biological responses are interrelated. Although dose can be estimated on the basis of exposure parameters and ozone concentration, such an approach ignores ozone absorption by the upper respiratory tract, and does not account for differences among individuals. Of particular interest has been the ability to measure the amount of ozone absorbed upstream (mouth, nose, and upper airways) of target respiratory tissues separately from the amount absorbed in the lower airways and acini.

Determining the respiratory dose of ozone requires an instrument that can (1) measure the ozone concentration at the airway opening, (2) respond with a dynamic response that is rapid relative to the subject's breathing frequency, (3) quantify ozone levels accurately at or below the National Ambient Air Quality Standard (NAAQS)*, and (4) provide measurements in both resting and exercizing subjects. The first analyzers developed for ozone dosimetry measurements had a relatively slow response time, which limited their practical application (Gerrity et al. 1988, 1995). As part of its research program to improve methods for assessing ozone dose to target tissues, HEI supported Dr. James Ultman and his collaborators to develop a rapidly responding analyzer to measure the absorption of inhaled ozone in the human respiratory tract (refer to Ultman and Ben-Jebria 1991 and Ultman et al. 1994 for additional background information). In their first two studies, the investigators made substantial technological advances by developing a chemiluminescent analyzer with a dynamic response time that was adequate for measuring ozone uptake at both low respiratory flow rates and relatively high ozone concentrations (higher than 0.5 ppm). However, that first-generation instrument was unable to measure ozone uptake at relevant ambient levels (0.07 to 0.20 ppm), and was not applicable to individuals engaged in moderate-to-strenuous physical activity. Therefore, HEI supported this third study with two objectives: (1) to redesign their first-generation ozone analyzer to have a faster response time and a lower ozone detection limit, and (2) to optimize the newly designed second-generation instrument by varying the operating parameters.

RATIONALE FOR THE STUDY

Previous work by Dr. Ultman and others (Gerrity et al. 1988, 1995) resulted in instruments that could measure ozone uptake in subjects with respiratory flow rates of less than 1,000 mL/sec, which is characteristic of low-to-moderate physical activity, and at exposure concentrations of greater than 0.5 ppm ozone (Ultman et al. 1994). Dr. Ultman's first-generation analyzer was able to continuously monitor ozone concentrations in air inspired and expired by human subjects after they inhaled a bolus of ozone (Ultman et al. 1994). That instrument had a number of limitations, including nonlinearity of the instrument calibration curve at low ozone levels, interference from expired carbon dioxide, a low signal-to-noise ratio (9:1) at 0.1 ppm ozone, and only a moderately rapid response time (110 msec). An instrument with improved ozone sensitivity and a faster response time relative to respiratory frequency was needed to determine the respiratory dose of ozone at ambient exposure levels and in exercising subjects.

OBJECTIVES AND STUDY DESIGN

The primary objective of this study was to improve the first-generation ozone analyzer that had been designed to noninvasively measure breath-to-breath ozone absorption in the human respiratory tract. The goals for the second-

* A list of abbreviations appears at the end of the Investigators' Report for your reference.

generation ozone analyzer were: (1) a response time of 50 msec; (2) decreased sensitivity to expired carbon dioxide; (3) increased sensitivity to permit linear measurement of ozone concentrations below 0.1 ppm; and (4) an increased signal-to-noise ratio of 30:1 at 0.1 ppm ozone. If these goals were achieved, the second-generation instrument would be capable of quantitatively measuring ozone uptake in human subjects engaged in moderate-to-strenuous physical activity while being exposed to ambient or near-ambient ozone levels.

The study was conducted in three phases. In Phase I, the investigators determined what conditions would permit near-optimal performance of the first-generation ozone analyzer (Ultman et al. 1994). Because the investigators had demonstrated earlier that ethylene reduced interference from carbon dioxide (Ben-Jebria and Ultman 1989), they modified their first-generation analyzer by replacing the ozone-reacting gas, 2-methyl-2-butene, with ethylene. This change improved the linearity of the calibration curve at ozone levels below 0.1 ppm and eliminated interference in the output signal caused by expired carbon dioxide. Knowing that ethylene has a slower reaction rate with ozone than 2-methyl-2-butene, the investigators increased the gas flow rate to compensate for the decreased reaction rate. The investigators tested the altered analyzer using both static calibration techniques and dynamic step-response methods until, in an intuitive process, they found a combination of operating parameters that would give the most rapid response time and the largest signal-to-noise ratio.

In Phase II, the investigators redesigned their first-generation analyzer, which originally consisted of five separate components. They mounted four of these components into a single cabinet in the second-generation instrument. The detector cell also was redesigned to improve mixing between reactant gas and ozone. These changes in the physical design improved the portability of the device, and ensured protection of its critical components, reduced electronic noise, and stabilized the thermal fluctuations of the analyzer.

In Phase III, the investigators tested the second-generation instrument, as they had in Phase I, by systematically varying each operating parameter, such as flow rate and reaction chamber pressure, to determine the optimal response time and signal-to-noise ratio. Optimization was achieved by a series of operating and electronic tests, and then the improved instrument was tested for carbon dioxide interference and for stability by determining its static calibration during six hours of continuous operation. Finally, they pilot-tested the performance of the second-generation ozone analyzer by measuring ozone uptake in two human subjects alternatively exposed to 0.11 ppm or 0.43 ppm ozone while at rest and while exercising.

TECHNICAL EVALUATION

ATTAINMENT OF STUDY OBJECTIVES

Dr. Ultman's study was thorough and comprehensive, and met most of the project's goals. Table 1 in this Commentary compares the performance characteristics of the second-generation ozone analyzer with those of the first-generation instrument.

METHODS AND STUDY DESIGN

The investigators applied a trial-and-error approach, rather than a statistical approach, to determine the optimal operating and electronic parameters; that is, certain parameters were held constant while others were varied. Although this approach may have resulted in the optimal solution, it does not guarantee that instrument optimization was achieved. A more technically appropriate approach would have been the use of statistical experimental design methods (Kuehl 1994; Deming 1978) to assure that the optimal combination of parameters had been found. However, to describe other features and properties of the second-generation analyzer, the investigators used statistical procedures that were appropriate for the type of data collected. Although only two human subjects were evaluated for ozone uptake by the second-generation analyzer, this portion of the study was intended only as a preliminary pilot test to validate the utility of the instrument with exercising subjects exposed to low ozone concentrations.

RESULTS AND INTERPRETATION

The investigators overcame two deficiencies of their first-generation ozone analyzer by changing the reactant gas from 2-methyl-2-butene to ethylene. This change minimized interference from carbon dioxide and allowed for the linear measurement of ozone at low concentrations. The investigators also reduced the instrument response time from 110 msec to 70 msec. This reduction, though significant, did not quite meet the goal of a 50-msec response time. In addition, the investigators were unable to markedly improve the signal-to-noise ratio. The ratio for the second-generation instrument was 11:1 at 0.1 ppm ozone, compared with the ratio of 9:1 for the first-generation analyzer and the project goal of 30:1. Nevertheless, because of the improved response characteristics, the second-generation ozone analyzer was able to measure ozone respiratory uptake in two subjects with breathing rates corresponding with moderate-to-strenuous physical activity while being exposed to a low level of ozone (0.11 ppm).

The second-generation analyzer was tested at levels that were both static (0.02 to 1 ppm) and dynamic (step changes of 0.1 ppm ozone over a range of ozone concentrations) to mimic the concentration changes encountered during breathing. The instrument's signal stability over six hours of operation was acceptable, although the baseline drifted slightly.

The investigators have discussed theoretical performance aspects of the detector in detail. They developed a mathematical model, which appears in Appendix A, to aid in evaluating the effects of various theoretical changes in instrument configuration, and explored several design changes that may result in further improvement to the instrument. For example, the theoretical model suggests that a decrease in reaction chamber volume should result in a shortened response time. However, reducing reaction chamber volume also decreases sensitivity and the signal-to-noise ratio. Further detector improvements may need to focus on ways to reduce the electronic noise of the instrument.

Instrument testing appears to have been sufficient except for one issue. Testing indicated that the fractional ozone uptake in two human subjects was approximately 0.8, regardless of the test conditions (i.e., respiratory frequency and ozone concentration). However, the investigators did not demonstrate the instrument's ability to measure fractional ozone uptake greater than 0.8. Although it is likely that 100% ozone absorption can be measured by the instrument, a positive control experiment demonstrating this feature would fully validate the analyzer's performance.

It is important to view the results of the pilot test with human subjects as preliminary; the goal of this portion of the study was to validate the instrument's usefulness with human subjects being exposed to ambient ozone levels while exercising, rather than to measure quantitatively the magnitude of ozone uptake in these subjects.

IMPLICATIONS FOR FUTURE RESEARCH

The improvements in analyzer performance in response time and signal-to-noise ratio at 0.1 ppm ozone fell short of the desired specifications. These will limit the use of the instrument to a maximal breathing rate of 30 breaths per minute at the specified exposure concentration. However, these conditions encompass most situations in which individuals are normally exposed to ozone. At lower breathing frequencies, this improved instrument would be able to measure lower ozone concentrations. Conversely, at higher breathing rates, a greater ozone concentration would be required for detection.

A few suggestions may be made regarding future changes to further improve detector performance. These include (1) using other reactant gases to decrease the response time; (2) cooling the instrument to improve its thermal stability and decrease the signal-to-noise ratio; and (3) reducing the inherent electronic noise of the instrument, which would improve the signal-to-noise ratio and allow for both a lower detection limit and a faster response time. The theoretical model suggests that design changes aimed at shortening the response time of the instrument are likely to be compromised by decreasing the signal-to-noise ratio, which would in turn result in decreased ozone sensitivity. Therefore, further design improvements will need to balance the impact of each alteration on other performance characteristics.

Table 1. Performance Characteristics of First-Generation and Second-Generation Ozone Analyzers

Parameter	Goal	First-Generation Instrument[a]	Second-Generation Instrument[b]
Response time (msec)	50	110	70
Signal-to-noise ratio at 0.1 ppm ozone	30:1	9:1	11:1
Minimal detectable ozone concentration (ppm)	< 0.12 in subjects during heavy exercise	0.5 in subjects at rest	0.11 in subjects during moderate exercise
Maximal respiratory rate (breaths/min)	> 30	< 30	~ 30
CO_2 interference	None	Some	None
Linear calibration at low ozone levels	Yes	No	Yes

[a] See Ultman and Ben-Jebria 1991 and Ultman et al. 1994 for full descriptions of the first-generation analyzer.

[b] This second-generation analyzer refers to the instrument described in the accompanying Investigators' Report.

The use of the instrument with subjects while exercising and being exposed to ambient ozone levels was validated in two human subjects. Therefore, this second-generation ozone analyzer should allow for more detailed human studies focused on the quantitative determination of respiratory ozone uptake in exercising subjects, and expand upon the existing theoretical ozone uptake model developed for resting subjects (Ultman et al. 1994).

CONCLUSIONS

The investigators redesigned and optimized a chemiluminescent ozone analyzer to measure ozone absorption in the respiratory tract. They minimized interference from expired carbon dioxide by changing the reactant gas from 2-methyl-2-butene to ethylene, which allowed the linear measurement of low ozone concentrations, and reduced the instrument's response time from 110 msec to 70 msec. Although the investigators were unable to alter the signal-to-noise ratio markedly, they extended the lower limit of the ozone observation range from 0.5 ppm to 0.1 ppm because of the analyzer's improved response characteristics.

Preliminary pilot studies demonstrated the second-generation ozone analyzer's ability to measure respiratory ozone uptake in human subjects with breathing rates corresponding to moderate-to-strenuous exercise while being exposed to a low ozone level (0.11 ppm). In its current configuration, the instrument is appropriate for exposure situations in which the subject's breathing frequency is less than 30 breaths per minute (corresponding to moderate-to-strenuous physical activity) at a minimum exposure concentration of 0.1 ppm ozone. Although further improvements are possible, this rapid-response ozone analyzer permits measurements of ozone uptake in exercising human subjects, without correcting for nonlinearity, carbon dioxide interference, or slow response time. By collecting this type of clinical data, experiments examining true dose-response relationships for ozone in humans should be possible.

ACKNOWLEDGMENTS

The Health Review Committee wishes to thank the ad hoc reviewers and Dr. Edo Pellizzari for their help in evaluating the scientific merit of the Investigators' Report, Dr. William Busby for coordinating the review process, and Dr. Diane Silverman for her assistance in preparing its Commentary. The Committee also acknowledges Virgi Hepner and Susan Shepard for their editorial assistance, Valerie Kelleher and Malti Sharma for overseeing the publication of this report, and Mary Stilwell for her administrative support.

REFERENCES

Bates DV. 1995. Ozone: A review of recent experimental, clinical and epidemiological evidence, with notes on causation, Part 1. Cancer Res 2:25–31.

Ben-Jebria A, Ultman JS. 1989. Fast-responding chemiluminescent ozone analyzer for respiratory applications. Rev Sci Instrum 60:3004–3011.

Deming SN, Morgan SL. 1978. Simplex Optimization: Course Notes. University of Houston, Houston, TX.

Gerrity TR, Biscardi F, Strong A, Garlington AR, Brown JS, Bromberg PA. 1995. Bronchoscopic determination of ozone uptake in humans. J Appl Physiol 79:852–860.

Gerrity TR, Weaver RA, Berntsen J, House DE, O'Neill JJ. 1988. Extrathoracic and intrathoracic removal of O_3 in tidal-breathing humans. J Appl Physiol 65:393–400.

Kuehl RO. 1994. Statistical Principles of Research Design and Analysis. Duxbury Press, Belmont, CA.

Lippmann M. 1989. Health effects of ozone: A critical review. J Air Pollut Control Assoc 39:672–695.

Lippmann M. 1993. Health effects of tropospheric ozone: Review of recent research findings and their implications to ambient air quality standards. J Expos Anal Environ Epidemiol 3:103–129.

Ultman JS, Ben-Jebria A. 1991. Noninvasive Determination of Respiratory Ozone Absorption: Development of a Fast-Responding Ozone Analyzer. Research Report Number 39. Health Effects Institute, Cambridge, MA.

Ultman JS, Ben-Jebria A, Hu S-C. 1994. Noninvasive Determination of Respiratory Ozone Absorption: The Bolus-Response Method. Research Report Number 69. Health Effects Institute, Cambridge, MA.

U. S. Environmental Protection Agency. 1996. Review of National Ambient Air Quality Standard for Ozone: Assessment of Scientific and Technical Information. OAQPS Staff Paper. EPA-452/R-96-007. Office of Air Quality Planning and Standards, Research Triangle Park, NC.

RELATED HEI PUBLICATIONS: OZONE AND DOSIMETRY

Report No.	Title	Principal Investigator	Publication Date
Ozone			
Research Reports			
1	Estimation of Risk of Glucose 6-Phosphate Dehydrogenase–Deficient Red Cells to Ozone and Nitrogen Dioxide	M. Amoruso	1985
3	Transport of Macromolecules and Particles at Target Sites for Deposition of Air Pollutants	T.T. Crocker	1986
6	Effect of Nitrogen Dioxide, Ozone, and Peroxyacetyl Nitrate on Metabolic and Pulmonary Function	D.M. Drechsler-Parks	1987
11	Effects of Ozone and Nitrogen Dioxide on Human Lung Proteinase Inhibitors	D.A. Johnson	1987
14	The Effects of Ozone and Nitrogen Dioxide on Lung Function in Healthy and Asthmatic Adolescents	J.Q. Koenig	1988
22	Detection of Paracrine Factors in Oxidant Lung Injury	A.K. Tanswell	1989
37	Oxidant Effects on Rat and Human Lung Proteinase Inhibitors	D.A. Johnson	1990
38	Synergistic Effects of Air Pollutants: Ozone Plus a Respirable Aerosol	J.A. Last	1991
44	Leukocyte-Mediated Epithelial Injury in Ozone-Exposed Rat Lung	K. Donaldson	1991
48	Effects of Ozone on Airway Epithelial Permeability and Ion Transport	P.A. Bromberg	1991
50	The Role of Ozone in Tracheal Cell Transformation	D.G. Thomassen	1992
60	Failure of Ozone and Nitrogen Dioxide to Enhance Lung Tumor Development in Hamsters	H. Witschi	1993
65	Consequences of Prolonged Inhalation of Ozone on F344/N Rats: Collaborative Studies		
	Part I: Content and Cross-Linking of Lung Collagen	J. Last	1994
	Part II. Mechanical Properties, Responses to Bronchoactive Stimuli, and Eicosanoid Release in Isolated Large and Small Airways	J.L. Szarek	1994
	Part III: Effects on Complex Carbohydrates of Lung Connective Tissue	B. Radhakrishnamurthy	1994
	Part IV: Effects on Expression of Extracellular Matrix Genes	W.C. Parks	1994
	Part V: Effects on Pulmonary Function	J.R. Harkema	1994
	Part VI: Background and Study Design	Project Staff	1995
	Part VII: Effects on the Nasal Mucociliary Apparatus	J.R. Harkema	1994
	Part VIII: Morphometric Analysis of Structural Alterations in Alveolar Regions	L-Y. Chang	1995
	Part IX: Changes in the Tracheobronchial Epithelium, Pulmonary Acinus, and Lung Antioxidant Enzyme Activity	K.D. Pinkerton	1995
	Part X: Robust Composite Scores Based on Median Polish Analysis	P.J. Catalano	1995
	Part XI: Integrative Summary	The Collaborative Ozone Project Group	1995
	Part XII: Atrophy of Bone in Nasal Turbinates	J.R. Harkema	1997

(Continued on next page)

Report No.	Title	Principal Investigator	Publication Date
70	Oxidant and Acid Aerosol Exposure in Healthy Subjects and Subjects with Asthma		1994
	Part I: Effects of Oxidants, Combined with Sulfuric or Nitric Acid, on the Pulmonary Function of Adolescents with Asthma	J.Q. Koenig	
	Part II: Effects of Sequential Sulfuric Acid and Ozone Exposures on the Pulmonary Function of Healthy Subjects and Subjects with Asthma	M.J. Utell	
71	Activation of Eicosanoid Metabolism in Human Airway Epithelial Cells by Ozonolysis Products of Membrane Fatty Acids	G.D. Leikauf	1995
75	Ozone Exposure and Daily Mortality in Mexico City: A Time-Series Analysis	D.P. Loomis	1996
HEI Communications			
1	New Methods in Ozone Toxicology: Abstracts of Six Pilot Studies		1992
3	Environmental Epidemiology Planning Project: Tropospheric Ozone Section		1994

Air Pollutant Dosimetry

Resesarch Reports

10	Predictive Models for Deposition of Inhaled Diesel Exhaust Particles in Humans and Laboratory Species	C.P. Yu	1987
28	Nitrogen Dioxide and Respiratory Infection: Pilot Investigations	J.M. Samet	1989
39	Noninvasive Determination of Respiratory Ozone Absorption: Development of a Fast-Responding Ozone Analyzer	J.S. Ultman	1991
40	Retention Modeling of Diesel Exhaust Particles in Rats and Humans	C.P. Yu	1991
45	The Effects of Exercise on Dose and Dose Distribution of Inhaled Automotive Pollutants	M.T. Kleinman	1991
58	Nitrogen Dioxide and Respiratory Illness in Infants		1993
	Part I: Health Outcomes	J.M. Samet	
	Part II: Assessment of Exposure to Nitrogen Dioxide	W.E. Lambert	
59	Noninvasive Methods for Measuring Ventilation in Mobile Subjects		1993
	Measurements of Ventilation in Freely Ranging Subjects	F.D. McCool	
	Assessment of Heart Rate As a Predictor of Ventilation	J.M. Samet	
63	Development of Samplers for Measuring Human Exposures to Ozone		1994
	Active and Passive Ozone Samplers Based on a Reaction with a Binary Regeant	J.D. Hackney	
	A Passive Ozone Sampler Based on a Reaction with Nitrate	P. Koutrakis	
	A Passive Ozone Sampler Based on a Reaction with Iodide	Y. Yanagisawa	
69	Noninvasive Determination of Respiratory Ozone Absorption: The Bolus-Response Method	J.S. Ultman	1994

Copies of these reports can be obtained by writing or calling the Health Effects Institute, 955 Massachusetts Avenue, Cambridge, MA 02139. Phone (617) 876-6700. FAX (617) 876-6709. E-mail pubs@healtheffects.org. www.healtheffects.org

HEI

The Board of Directors

Archibald Cox *Chairman*
Carl M. Loeb University Professor (Emeritus), Harvard Law School

Douglas Costle
Chairman of the Board and Distinguished Senior Fellow, Institute for Sustainable Communities

Alice Huang
Dean of Science, New York University

Donald Kennedy
President (Emeritus) and Bing Professor of Biological Sciences, Stanford University

Susan B. King
Fellow, Sanford Institute of Public Policy, Duke University

Richard B. Stewart
Professor, New York University School of Law

Robert M. White
President (Emeritus), National Academy of Engineering, and Senior Fellow, University Corporation for Atmospheric Research

Health Research Committee

Bernard D. Goldstein *Chairman*
Director, Environmental and Occupational Health Sciences Institute

Glen R. Cass
Professor of Environmental Engineering and Mechanical Engineering, California Institute of Technology

Seymour J. Garte
Professor, Department of Environmental Medicine, New York University Medical Center

Leon Gordis
Professor, Department of Epidemiology, Johns Hopkins University, School of Hygiene and Public Health

Rogene Henderson
Senior Scientist, Lovelace Respiratory Research Institute

Meryl H. Karol
Professor of Environmental and Occupational Health, University of Pittsburgh Graduate School of Public Health

Robert F. Sawyer
Class of 1935 Professor of Energy (Emeritus), University of California at Berkeley

Frank E. Speizer
Edward H. Kass Professor of Medicine, Channing Laboratory, Harvard Medical School, Department of Medicine, Brigham and Women's Hospital

Gerald van Belle
Chairman, Department of Environmental Health, School of Public Health and Community Medicine, University of Washington

Health Review Committee

Arthur Upton *Chairman*
University of Medicine and Dentistry of New Jersey–Robert Wood Johnson Medical School and Environmental and Occupational Health Sciences Institute

John C. Bailar III
Chair, Department of Health Studies, Biological Sciences Division, University of Chicago

A. Sonia Buist
Professor of Medicine and Physiology, Oregon Health Sciences University

Ralph D'Agostino
Professor of Mathematics/Statistics and Public Health, Boston University

Thomas W. Kensler
Professor, Division of Toxicological Sciences, Department of Environmental Sciences, Johns Hopkins University

Donald J. Reed
Professor and Director, Environmental Health Sciences Center, Oregon State University

David J. Riley
Professor of Medicine, University of Medicine and Dentistry of New Jersey–Robert Wood Johnson Medical School

Robert M. Senior
Dorothy R. and Hubert C. Moog Professor of Pulmonary Diseases in Medicine, Washington University School of Medicine

Officers and Staff

Daniel S. Greenbaum *President*
Richard M. Cooper *Corporate Secretary*
Howard E. Garsh *Director of Finance and Administration*
Kathleen M. Nauss *Director for Scientific Review and Evaluation*
Robert M. O'Keefe *Director of Program Strategy*
Jane Warren *Director of Research*
Aaron J. Cohen *Senior Scientist*
Maria G. Costantini *Senior Scientist*
Debra A. Kaden *Senior Scientist*
Bernard Jacobson *Staff Scientist*
Martha E. Richmond *Staff Scientist*
Geoffrey H. Sunshine *Staff Scientist*
Gail V. Allosso *Senior Administrative Assistant*
L. Virgi Hepner *Managing Editor*
Kevin Jenkins *Administrative Assistant*
Valerie Kelleher *Publications Production Coordinator*
Francine Marmenout *Administrative Assistant*
Teresina McGuire *Accounting Assistant*
Beverly Morse *Receptionist*
Jacqueline C. Rutledge *Controller*
Malti Sharma *Publications Assistant*
Mary L. Stilwell *Administrative Assistant*

HEI HEALTH EFFECTS INSTITUTE 955 Massachusetts Avenue, Cambridge, MA 02139 (617) 876-6700

Research Report Number 79 October 1997